



UNIVERSIDADE FEDERAL DO PARÁ
INSTITUTO DE GEOCIÊNCIAS
CURSO DE PÓS-GRADUAÇÃO EM GEOFÍSICA

MASTER DEGREE DISSERTATION

**Joining diffraction filter and residual diffraction
moveout to construct a velocity model in the depth
and time domains: application to a Viking Graben
data set**

JAIME ANDRES COLLAZOS GONZALEZ

Belém
2014

JAIME ANDRES COLLAZOS GONZALEZ

**Joining diffraction filter and residual diffraction
moveout to construct a velocity model in the depth
and time domains: application to a Viking Graben
data set**

Dissertation submitted to the Postgraduate Program in
Geophysics of the Universidade Federal do Pará for ob-
taining a Master's Degree in Geophysics.

Concentration area: Seismic methods

Advisor: José Jadsom Sampaio de Figueiredo

Belém
2014

Dados Internacionais de Catalogação de Publicação (CIP)
Biblioteca do Instituto de Geociências/SIBI/UFPA

Collazos González, Jaime Andrés, 1985-

Joining diffraction filter and residual diffraction moveout to construct a velocity model in the depth and time domains: application to a Viking Graben data set / Jaime Andrés Collazos González. – 2014.

36 f. : il. ; 30 cm

Inclui bibliografias

Orientador: José Jadsom Sampaio de Figueiredo

Dissertação (Mestrado) – Universidade Federal do Pará, Instituto de Geociências, Programa de Pós-Graduação em Geofísica, Belém, 2014.

1. Diffraction patterns - Data processing. 2. Seismological imaging systems. 3. Seismic reflection method. I. Title.

CDD 22. ed. 621.36

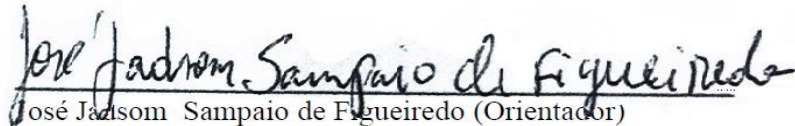
JAIME ANDRES COLLAZOS GONZALEZ

**Joining diffraction filter and residual diffraction
moveout to construct a velocity model in the depth
and time domains: application to a Viking Graben
data set**

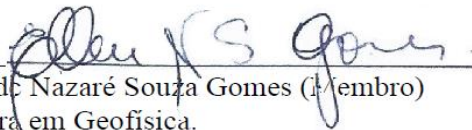
Dissertation submitted to the Postgraduate Program in
Geophysics of the Universidade Federal do Pará for ob-
taining a Master's Degree in Geophysics.

Approval date: August 14, 2014

Examining committee:



José Jadsom Sampaio de Figueiredo (Orientador)
Doutor em Ciências e Engenharia de Petróleo.
Universidade Federal do Pará.



Ellen de Nazaré Souza Gomes (Membro)
Doutora em Geofísica.
Universidade Federal do Pará.



Jorg Schleicher (Membro)
Doutor em Geofísica.
Universidade Estadual de Campinas.

In memory to my grandfather Angelino Gonzalez who always infused me discipline to reach my goals. I know he still cares for me. To my son Angel who means everything in my life. . .

ACKNOWLEDGMENTS

To my mother Lucrecia who teach me everything what I need for live, to my mother Bellanir who left behind her dreams for follow my own dreams, to my aunt Elcy who filled my days with lovely words, to my uncle Elver who has been my father, my friend and my buddy, to my uncle Dago who gives me support in every choice, to my brother Oscar and all the family.

To my wife and my son, Katherine and Angel who are the center of my life, thanks to them I feel the real happiness, they are the reason for me to reach my goals.

To my family in law for loving me like another member the Rincon Perez family, and to be with me in the distance. To my Father Jaime and the Collazos Family for giving me support in the hard moments.

To my advisor Dr. José Jadsom for his valuable guidance doing this dissertation. To Dr Ellen Gomes for her endeavor and believe in my professionals skills and for giving me the opportunity for do this master. To all administrative staff, professors and partners particularly Carlos Alexandre, Fransisco and Zoraida from CPGF. I am grateful to all the persons around me for their direct or indirect contributions to this this project.

I would like to thank ExxonMobil for providing the Viking Graben data set. This work was kindly supported by the Brazilian agencies CAPES, FINEP, INCT-GP, and CNPq, as well as Petrobras and the sponsors of the Wave Inversion Technology (WIT) Consortium.

RESUMO

Ondas sísmicas difratadas são geradas por descontinuidades na subsuperfície da Terra com o tamanho da ordem do comprimento de onda sísmico. Uma vez que o campo de onda incidente pode ser significativamente afetado por essas descontinuidades, muitas propriedades importantes destes eventos podem ser usadas para melhorar a prática de imageamento sísmico. Neste trabalho propomos uma abordagem prática para construir modelos de velocidade no domínio do tempo e profundidade usando difrações. Esta metodologia consiste na aplicação do filtro destrutor de onda plana (plane wave destruction - PWD) juntamente com método residual diffraction moveout (RDM), de modo a construir modelos de velocidade nos domínios do tempo e da profundidade. Nosso método depende apenas de difrações (identificadas) filtradas a partir de eventos de reflexão e um modelo de velocidade inicial arbitrário de entrada. As imagens migrada no domínio pós-empilhado (nos domínios do tempo e da profundidade) são comparados com imagens migradas derivadas do processamento sísmico convencional. Nestes domínios, usamos a migração Kirchhoff pós-empilhamento. Desconsiderando a necessidade de identificar e escolher os eventos de difração na migração pós-empilhamento no domínio da profundidade, o método apresenta um custo computacional muito baixo. Para alcançar um modelo de velocidade aceitável o tempo de processamento comparado ao método convencional foi menor. A viabilidade de nossa metodologia é testado num dado sísmico real do Viking Graben.

Palavras-chaves: Sobretempo normal de difrações. Filtro de difrações. Remigração. Migração Pós-empilhamento. Tempo. Profundidade.

ABSTRACT

Diffracted seismic waves are generated by unsmooth structures in the subsurface with a size on the order of seismic wavelengths. Because the incident wavefield can be significantly affected by these discontinuities, many important properties of the seismic events can be used to improve the velocity model building. In this thesis, we propose a practical approach to construct velocity models in the time and depth domains using diffractions. This methodology applies the plane wave destruction (PWD) filter jointly with the residual diffraction moveout (RDM) method to construct velocity models in time and depth domains. Our method does not depend on any requirements except for identifiable diffractions filtered from reflection events and an arbitrary initial velocity model as input. The post-stack migrated images (in the time and depth domains) are compared with the migrated images derived from conventional seismic processing steps. In both cases, we used post-stack Kirchhoff Migration. Beyond the need to identify and select the diffraction events in the post-stack migrated sections in the depth domain, the method has a very low computational cost of processing time. To reach an acceptable velocity model was less compared with conventional processing. The applicability of our methodology was verified using a real Viking Graben seismic dataset.

Keywords: Diffraction Moveout. Diffraction Filtering. Remigration. Post-stack Migration. Time. Depth.

LIST OF FIGURES

2.1	(a) Synthetic Sigsbee2B data set. (b) Local slopes panel. (b) Diffraction section after application PWD.	17
2.2	The velocity model with a scattering point and Remigration trajectories.	19
2.3	The flowchart of RDM processing on real data.	21
2.4	The flowchart of RDM processing for a first iteration required.	22
2.5	The flowchart of RDM processing in case of nth iterations required.	23
3.1	The conventional velocity analysis	25
3.2	Conventional processing. The RMS velocity model.	25
3.3	Conventional processing. The NMO stacked section.	26
3.4	The PWD filter applied on ZO section. (a) Local slopes panel. (b) Diffraction section.	28
3.5	The RDM processing applied on ZO section. (a) The depth migration after apply PDW filter. (b) Remigration trajectories on undermigrated diffractions.	29
3.6	The RDM processing applied on ZO section. The RMS velocity model.	30
3.7	The RDM processing applied on ZO section. The time migration section.	31
3.8	Near-offset section	33
3.9	First iteration of RDM processing. (a) Local slopes of a near offset section. (b) Diffraction section.	34
3.10	First iteration of RDM processing. (a) Depth migrated with the PWD filter. (b) Undermigrated filtered diffractions	35
3.11	First iteration of RDM processing. RMS Velocity model.	36
3.12	First iteration of RDM processing. NMO stacked section.	37
3.13	Results from second iteration of RDM processing. (a) Local slopes panel of NMO stacked section. (b) Diffraction section, i.e. result of PWD filter applied to the NMO stacked section.	38
3.14	Second iteration of RDM processing. (a) Depth migration of diffraction section. (b) Undermigrated diffraction curves with remigration trajectories.	39
3.15	RMS velocity model from second iteration of RDM processing.	40
3.16	NMO stacked section from second iteration of RDM processing.	41
3.17	Time migrated sections. (a) Conventional processing. (b) RDM processing.	43
3.18	Final depth velocity models from (a) conventional and (b) RDM processing.	44
3.19	Depth migrated sections from (a) conventional processing and (b) RDM processing.	46

LIST OF ABBREVIATIONS

ABREVIATURA	DESCRIÇÃO
AGC	From english “Automatic Gain Control”
CMP	From english “Common Midpoint”
CRS	From english “Common Reflection Surface”
NMO	From english “Normal Move Out”
PWD	From english “Plane Wave Destruction”
RDM	From english “Residual Diffraction Move Out”
RMS	From english “Root Mean Square)”
SSA	From english “Singular Spectrum Analysis”
ZO	From english “Zero Offset”

LIST OF SYMBOLS

SYMBOL	DESCRIPTION
a	Semi-major axis of a hyperbola
b	Semi-minor axis of a hyperbola
σ	Local slope
P	Waveform
q	Inverse of local slope
v_0	Migration velocity
v_t	True velocity migration
v_t	True velocity migration
W	Windows around of the point

1 INTRODUCTION	13
2 METHODOLOGY	15
2.1 PWD FILTER AND LOCAL SLOPE	15
2.2 RDM ANALYSIS	18
2.3 RDM PROCESSING STEPS	19
3 RESULTS	24
3.1 DATASET DESCRIPTION AND PREPROCESSING	24
3.2 CONVENTIONAL VELOCITY ANALYSIS	24
3.3 RDM APPLICATION ON A CONVENTIONAL NMO STACKED SECTION	27
3.4 RDM PROCESSING ON NEAR OFFSET SECTION	32
4 CONCLUSIONS	48

Bibliography

1 INTRODUCTION

It is well known that when seismic waves interact with small structures in the subsurface of the earth (e.g., faults, fractures, channels, and rough edges of salt bodies), waves are scattered in all directions. The typical scattered signatures, known as diffractions, have been investigated for a long time with the purpose of understanding the signatures and how they might be used in seismic processing. The special features exhibited by diffraction signatures (hyperbola) have been particularly useful in the application of diffractions in velocity analysis (Sava et al., 2005; Fomel et al., 2007; Novais et al., 2008; Landa & Reshef, 2009; Coimbra et al., 2013), super-resolution (Khaidukov et al., 2004), linear fracture imaging (Alonaizi et al., 2013) and CO_2 time-lapse monitoring (Alonaizi et al., 2014).

Reflections and diffractions are two types of coherent events generated from the subsurface. However, in a conventional processing, most time is spent on reflections, and diffractions are considered noise due to their weak seismic energy. A conventional processing distorts the shape of a diffraction; thus, the true information about the structure generated by this wave type (Zhang, 2004) is lost most of time. Therefore, it is recommended to separate diffractions from reflections before any further analysis.

Although many studies have been dedicated to separating the diffractions from reflections and using their signatures in seismic processing, many challenges are still present and must be overcome. Recently, different studies have concentrated on separating diffractions from reflections. Khaidukov et al. (2004) proposed to mute the reflections by focusing and defocusing the residual wave-field in a shot gather that contains mostly shot diffractions. Asgedom et al. (2011) used the common reflection surface (CRS) concept to suppress the reflections, through the selection of an appropriate stacking surface for diffractions based on a coherency measurement named MUSIC. Klovov & Fomel (2013) used radon transform to separate diffractions from reflections in the dip-angle domain. Liu et al. (2013) proposed the singular spectrum analysis (SSA) method, which removes diffractions from the full wave field by taking advantage of the difference between the kinematic and dynamic properties of reflections and diffractions. Using the difference of these properties, Landa et al. (1987), Landa & Keydar (1998) developed methods to locate the diffraction points in the time domain and de Figueiredo et al. (2013) in the depth domain.

In this work, we performed a velocity analysis on seismic panels with diffractions filtered. In the first step, we implemented a diffraction filter based on the plane wave destruction (PWD) (Clearbout, 1992; Fomel, 2009) and the local slope approach developed by Schleicher et al. (2009). who use the local slope to carry out the PWD with a simple correction to the linear plane-wave destruction, based on the fact that its inverse can be extracted from the data in a fully analogous way. Combining the information of the slope

and its inverse can yield a simple but effective correction to the local slope. To separate the diffraction, we used the smooth variations of the slope.

In the second step, we performed a velocity analysis with the diffractions filtered. Our velocity analysis was performed based on the Residual Diffraction Moveout (RDM) technique developed by Coimbra et al. (2013). The method was developed for a zero offset dataset in the depth domain. Here, we applied it to a near offset (different from ZO). There is an error when applying the Coimbra et al. (2013) method on a non-zero offset section. However, as the method is iterative, the error is overcome after a couple of iterations. The number of iterations is dependent on the complexity of the data set. Finally, we compared the migrated seismic images (in time and depth domains) obtained by the conventional seismic processing with those obtained by the processing using RDM (in this case we will refer to it as RDM processing). The applicability of our analysis was verified using the real Viking Graben seismic dataset.

2 METHODOLOGY

In this section, we describe our methodology for the analysis based on the residual diffraction moveout (RDM) processing. Our unconventional seismic processing makes use of the plane wave destruction (PWD) filter to separate diffractions from reflections in near offset sections before application of RDM method. After separation, we use the residual moveout of an incorrectly migrated diffraction event in the depth domain to update of velocity model. Although the theory is developed for zero-offset sections, we assume that the error produced by the application to a near-offset section is corrected along the processing after some iterations.

2.1 PWD FILTER AND LOCAL SLOPE

The residual diffraction moveout (RDM) method uses the information of incorrectly migrated diffractions to determine the true velocity of the medium. However, it is well known, that reflection energy is dominant relatively to diffraction energy. Therefore, it is necessary to separate or attenuate the reflections with respect to diffraction, if we want to use diffractions in seismic processing. According to Clearbout (1992), plane-wave destruction (PWD) can be used to attenuate the almost planar events associated with a reflection. In Clearbout (1992) PWD is defined as the local plane differential given by,

$$\frac{\partial P}{\partial x} + \sigma \frac{\partial P}{\partial t} = 0, \quad (2.1)$$

where P is the wavefront that depends on offset x , time t , and the local slope parameter σ . However, according to the equation 2.1, to implement the PWD, we need to estimate σ . If we consider smooth variation of local slope to reflection and high lateral variation to diffraction, we can estimate and to apply the equation 2.1, just to the points in the seismic image that have little lateral variation, in this way, the residual of equation 2.1 is a diffraction seismic image. To determine this seismic parameter, there are several methods, such as the one described by Clearbout (1992), suggested an iterative method to find residual or data does not satisfy equation 2.1. Fomel (2009) implemented an all pass filter to find a similar solution using the finite difference of equation 2.1 in frequency domain, although this process required high computational resources. In our case, we used the method from Schleicher et al. (2009) to estimate of σ and the quadratic residual $R(\sigma)$ given by,

$$R(\sigma) = \sum_{i,j}^W \left(\frac{\partial P(x_i, t_j)}{\partial x} + \sigma \frac{\partial P(x_i, t_j)}{\partial t} \right)^2. \quad (2.2)$$

In the interesting work of Schleicher et al. (2009), was rewritten equation 2.2 (the technique applied by Clearbout (1992)) in order to estimate an inverse of σ . This approach is given by,

$$R(q) = \sum_{i,j}^W \left(q \frac{\partial P(x_i, t_j)}{\partial x} + \frac{\partial P(x_i, t_j)}{\partial t} \right)^2, \quad (2.3)$$

where W is the size of the window selected around point (x_i, t_j) . Equations 2.2 and 2.3 can be combined to give a simple and effective correction of the local slope. According to Schleicher et al. (2009), the least-squares solution to this problem is given by,

$$\langle \sigma \rangle_E = S \left(\sqrt{\frac{\sum_{i,j}^W \left(\frac{\partial P(x_i, t_j)}{\partial x} \right)^2}{\sum_{i,j}^W \left(\frac{\partial P(x_i, t_j)}{\partial t} \right)^2}} \right), \quad (2.4)$$

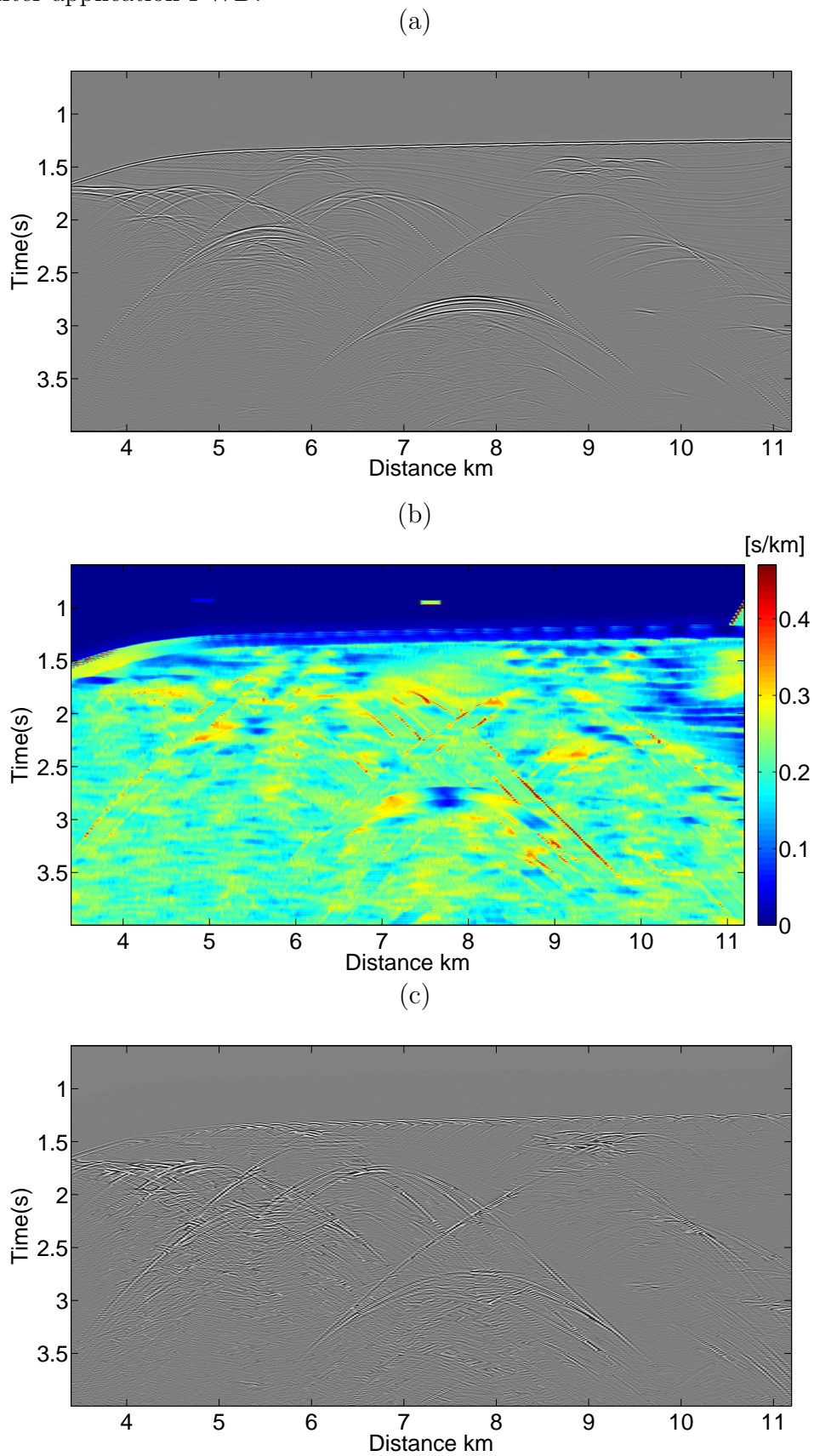
where S is defined as

$$S = -sgn \left(\sum_{i,j}^W \left(\frac{\partial P(x_i, t_j)}{\partial x} \right) \left(\frac{\partial P(x_i, t_j)}{\partial t} \right) \right). \quad (2.5)$$

Equation 2.4 minimizes the error of the least squares solution of equations 2.2 and 2.3. To implement of equation 2.1, any method can be used to estimate the slope, as long as a good estimate of this seismic parameter can be obtained.

We performed a initial tests with PWD filter in controlled synthetic data before used in real data. Figure 2.1a is the synthetic data (Sigsbee2B) used to test our PWD filter implementation. Figure 2.1b is the estimation of local slopes and Figure 2.1c is synthetic data after apply the PWD filter. We can observe at Figure 2.1c, that the energy of planar event is quite attenuated. In others word we can see a diffraction section panel.

Figure 2.1: (a) Synthetic Sigsbee2B data set. (b) Local slopes panel. (b) Diffraction section after application PWD.



Source: from author

2.2 RDM ANALYSIS

Recently, Coimbra et al. (2013) proposed a method for diffraction-point imaging and local migration velocity improvement based on the localization and picking of the residual moveout of incorrectly migrated diffraction events in depth domain. Here, we applied the Coimbra et al. (2013) methodology to construct velocity models in the depth and time domains.

According to Coimbra et al. (2013), considering a diffracting point at the true position (x_t, z_t) in a constant-velocity medium with true velocity v_t , the residual moveout of a diffraction event after of depth migration with an incorrect velocity v_0 is the Huygens image-wave for the depth remigration from velocity v_t to v_0 (Hubral et al., 1996a). These authors defined the location of the Huygen's image-wave as the curve or surface of all points where a possible event at the image point (x_t, z_t) might be placed when the migration velocity is changed from v_t to v_0 . That is, if the migration velocity is higher than the medium velocity, the overmigrated diffraction events will have the shapes of ellipses or if the migration velocity is smaller, the shapes of the undermigrated diffraction events are hyperbolas. (Hubral et al., 1996b) show that the Huygen's image-wave is given by,

The construction of this curve is defined as,

$$\frac{z^2}{v_0^2} + \frac{(x - x_t)^2}{v_0^2 - v_t^2} = \frac{z_t^2}{v_t^2}. \quad (2.6)$$

However, the preferred parameters to describe a hyperbola or an ellipse are the half-axes (a and b). Therefore, Coimbra et al. (2013) rewrite equation 2.6 in the form,

$$\frac{z^2}{b^2} + s \frac{(x - x_t)^2}{a^2} = 1, \quad (2.7)$$

where the half-axes a and b are given by,

$$a = \frac{z_t}{v_t} \sqrt{|v_0^2 - v_t^2|} \quad \text{and} \quad b = \frac{z_t}{v_t} v_0 \quad (2.8)$$

Depending on the sign $s = \text{sgn}(v_0^2 - v_t^2) = \text{sgn}(v_0 - v_t)$ equation 2.7 can represent an ellipse or a hyperbola.

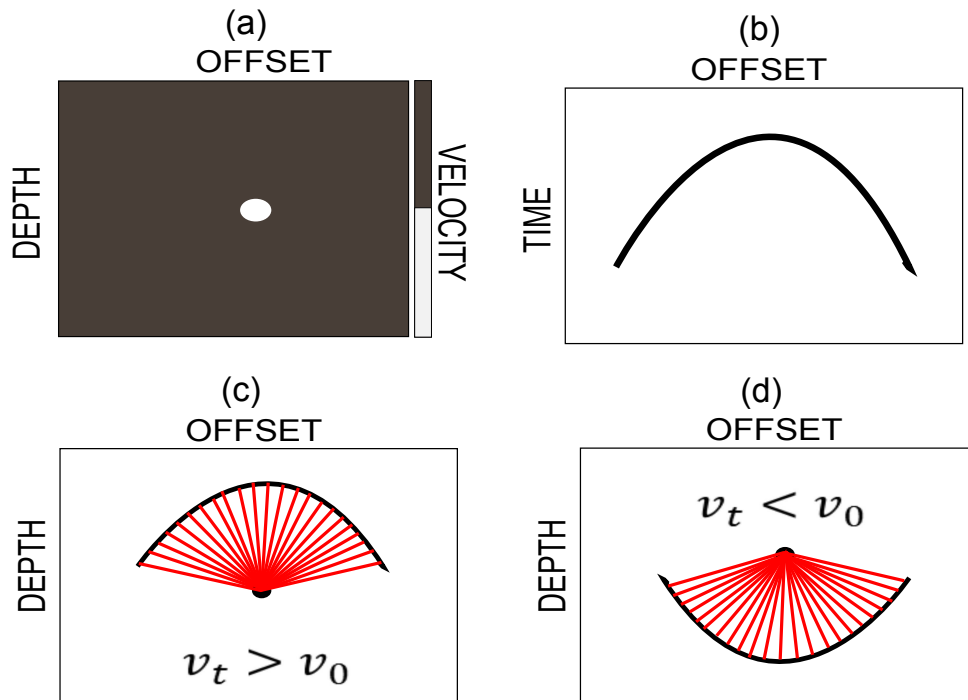
Coimbra et al. (2013) used a least-squares method to find the best-fitting hyperbola to describe an undermigrated diffraction event or the best-fitting ellipse for an overmigrated diffraction event. This provides an estimation for the half-axes (a) and (b) as the horizontal coordinate of the apex x_t . In other words, the (a) and (b) parameters are related to the slope of incorrectly migrated diffractions. In a medium with a strong velocity gradient this slope can be quite affected.

The residual moveout of the incorrectly migrated diffraction events can be used to update the migration velocity model. According to Coimbra et al. (2013) there are two

ways to update the velocity model. One of them is related to the half-axes and the other one is using remigration trajectories (for example, the red curves show in Figure 2.2c and 2.2d).

Figure 2.2 shows a pictorial illustration of incorrectly migrated diffractions curves (black lines) with remigration trajectories (red lines). The black lines in Figure 2.2c and 2.2d are the hyperbola and ellipse curves described by equations 2.7 e 2.8.

Figure 2.2: (a) Constant velocity model background with a scattering point located at center of model. (b) Zero-offset section over a diffraction point. (c) Remigration trajectories (red line) starting at a hyperbolic migrated diffraction curve (black line). (d) Remigration trajectories (red line) starting at an elliptic migrated diffraction curve (black line).



Source: from author

According to Hubral et al. (1996b) the remigration trajectories are the approach of remigration image-wave equation, to find ray-like trajectories. These remigration trajectories are all position of a diffraction that can be found in a migrated image as a function of migration velocity. More detail about the RDM method can be found at Coimbra et al. (2013).

2.3 RDM PROCESSING STEPS

The RDM processing sequence consists of the following steps:

- 1) Pre-processing (geometry correction, trace editing, deconvolution, band-pass fil-

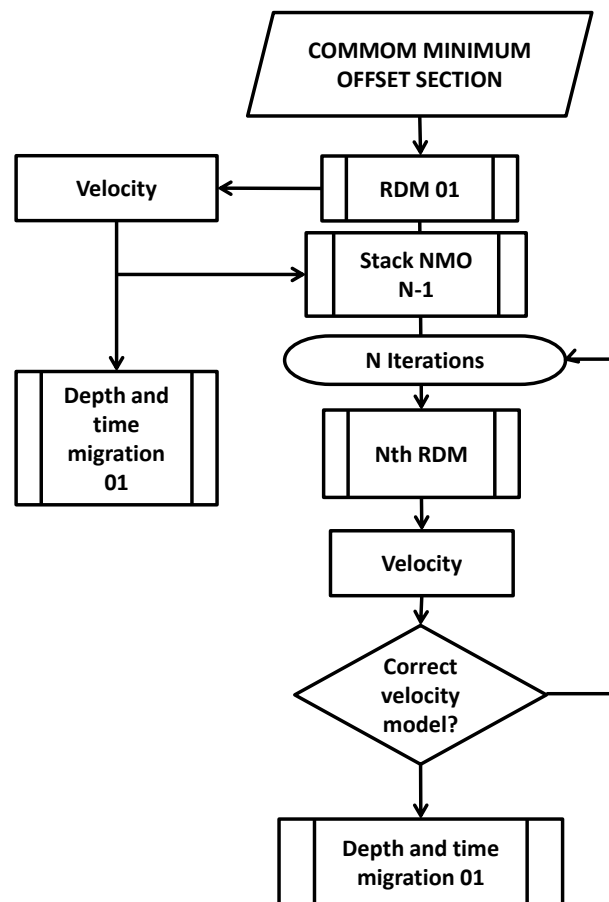
tering and AGC) of real data set. This work was performed for the conventional and unconventional velocity analyses.

- 2) Selecting the near-offset gather from the real data set.
- 3) Calculating the local slope for the near offset section.
- 4) Applying the PWD filter to separate diffractions from reflections.
- 5) Performing the migration of filtered diffractions using a constant velocity model with $v = 1500m/s$ in the first iteration and from the second iteration use the velocity model found in the preview iteration.
- 6) Applying the RDM processing on this gather to find the first velocity model.
- 7) Applying NMO with this velocity model on the data set to obtain the first ZO section.
- 8) Using this first ZO section as the input to the next iteration.
- 9) Iterative steps 3 to 8 until velocity models satisfactory.

Note that we applied the steps shown above, to the Viking Graben dataset. Only two iteration were necessary for convergence. Other data maybe require more than two iterations to achieve a reasonable velocity model for migration. That is, the number of iterations required will depend on the complexity of the data.

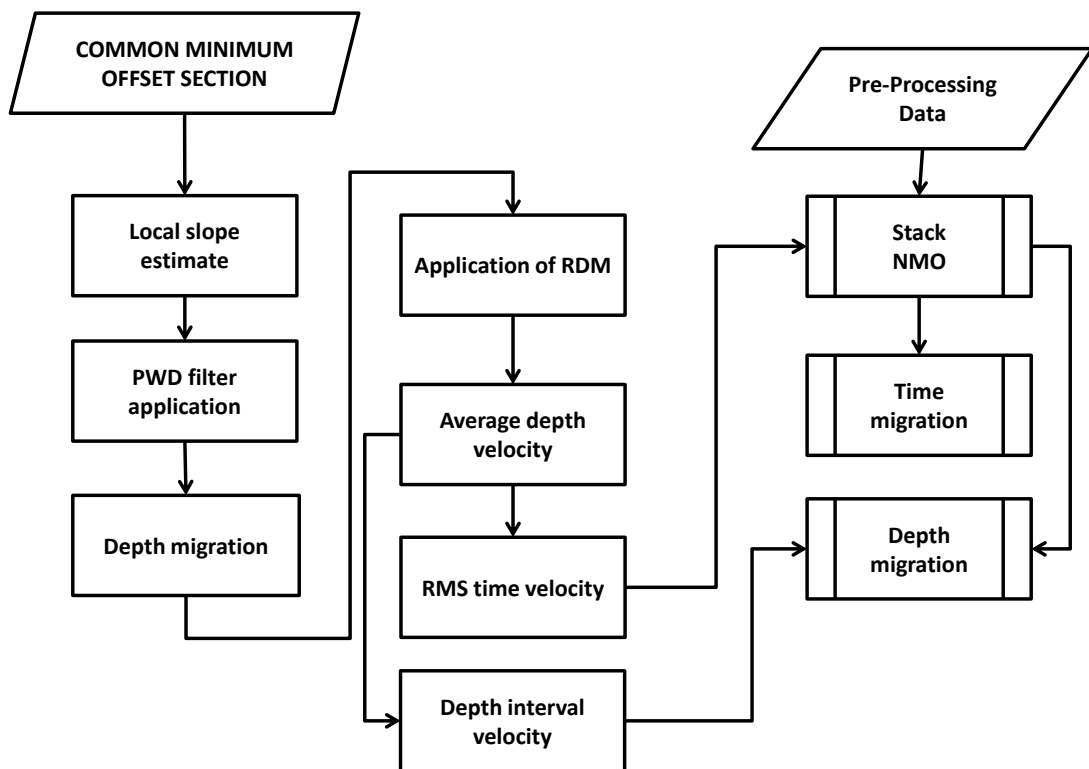
The new RDM processing to construct a velocity model, starting from a near offset section, applies the PWD filter to separate diffraction events, and applies the residual diffraction moveout method to obtain a velocity model. The steps are described in Figures 2.3, 2.4 and 2.5.

Figure 2.3: The flowchart of RDM processing on real data.



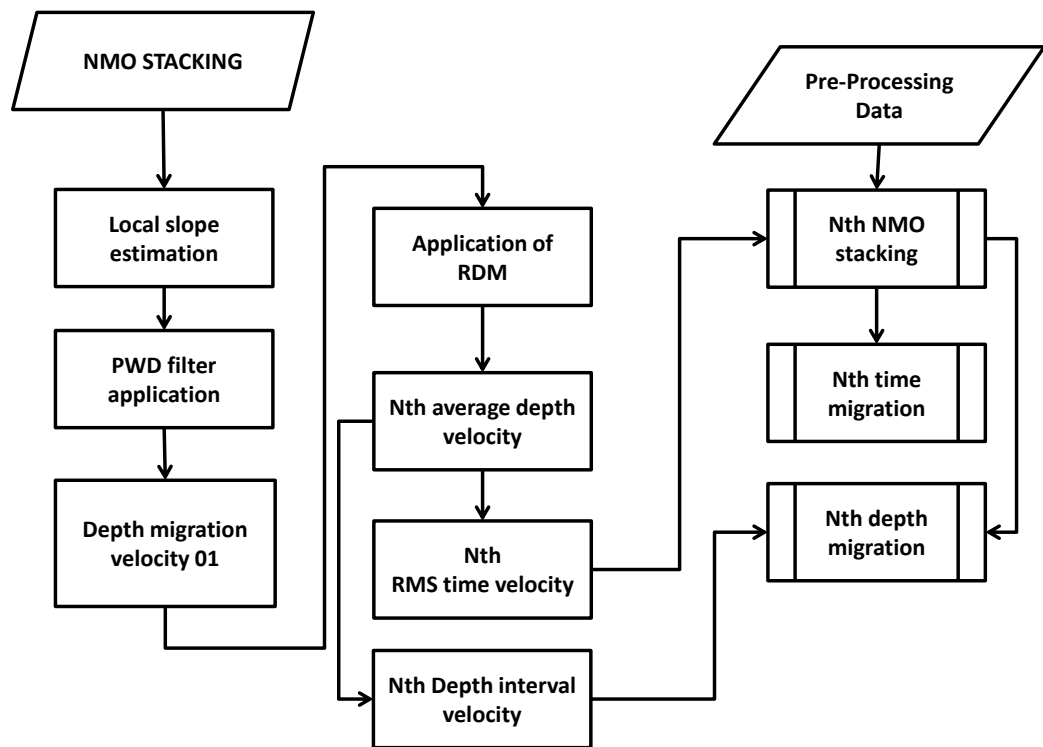
Source: from author

Figure 2.4: The flowchart of RDM processing for a first iteration required.



Source: from author

Figure 2.5: The flowchart of RDM processing in case of nth iterations required.



Source: from author

3 RESULTS

In this work, we have applied our new seismic processing methodology to a real data set (a Viking Graben dataset from the North Sea Basin) provided by Exxon Mobil.

3.1 DATASET DESCRIPTION AND PREPROCESSING

The Viking Graben data set was acquired with 1001 shot points and 120 channels. The sampling rate was 4 ms and the recording time was 6 s. The distance was 25 m between the shot points and 25 m between the receivers. The minimum and maximum offsets were 262 and 3237 m respectively. The water depth along the seismic line was a relatively constant value of 300 m. This data set needed a seismic pre-processing to enhance the data and to attenuate the noise before applying our methodology. However, because of a large number of diffractions, the data set is good for an application of the RDM method. That is, to successfully apply our method, the data must contain many diffractions. In geological terms, this means more faults and discontinuities in the subsurface.

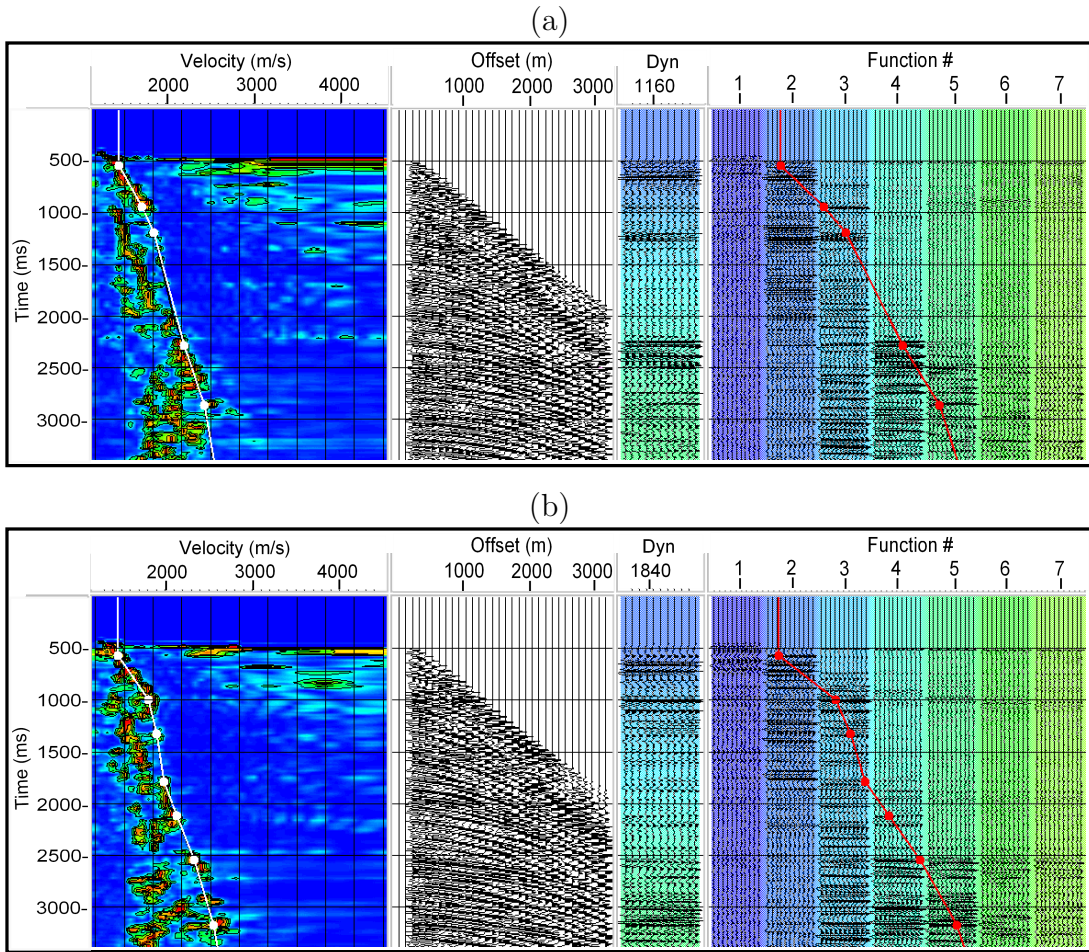
The pre-processing and processing steps consisted of: trace muting, bandpass filtering with a zero-phase (6-12-50-70) Hz Ormsby filter, spherical divergence corrections, and predictive deconvolution with 320 ms of operator length and 20 ms prediction operator. Here, we also used a deconvolution with white noise ($S/N=0.1$) and a predictive deconvolution to improve the amplitude resolution.

3.2 CONVENTIONAL VELOCITY ANALYSIS

In this step, we performed a conventional processing of the Viking Graben data set to obtain a post-stack time migration and post-stack depth migration images and the corresponding velocity models as a reference for the comparison with the results from application of the RDM method (as mentioned before, we call this operation the RDM processing). To compare with other seismic images of Viking Graben, we used the time migration image of Gislain & McMechan (2003).

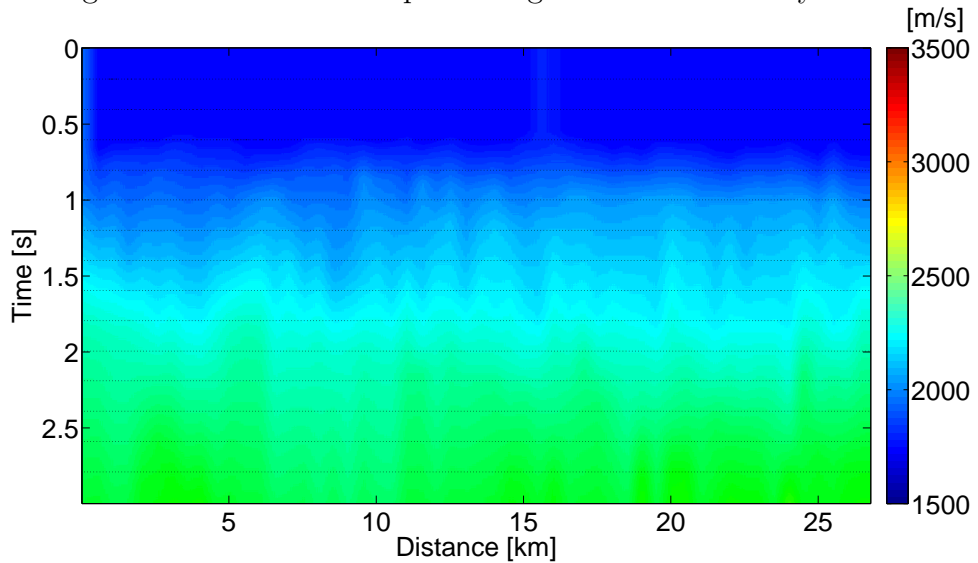
Conventional NMO velocity analysis was performed at every 50 midpoints using velocity spectra ranging from 1500 to 3000 m/s. Figure 3.1 shows the semblance velocity analysis from CMP 1163 and CMP 1843. The velocity model was created by interpolation and the stacked used the normal moveout correction. After the analysis, we performed a second velocity analysis to improve the NMO correction. Figure 3.2 shows the RMS velocity model and Figure 3.3 the NMO stacked section from conventional processing.

Figure 3.1: The conventional velocity analysis for (a) CMP 1163 and (b) CMP 1843.



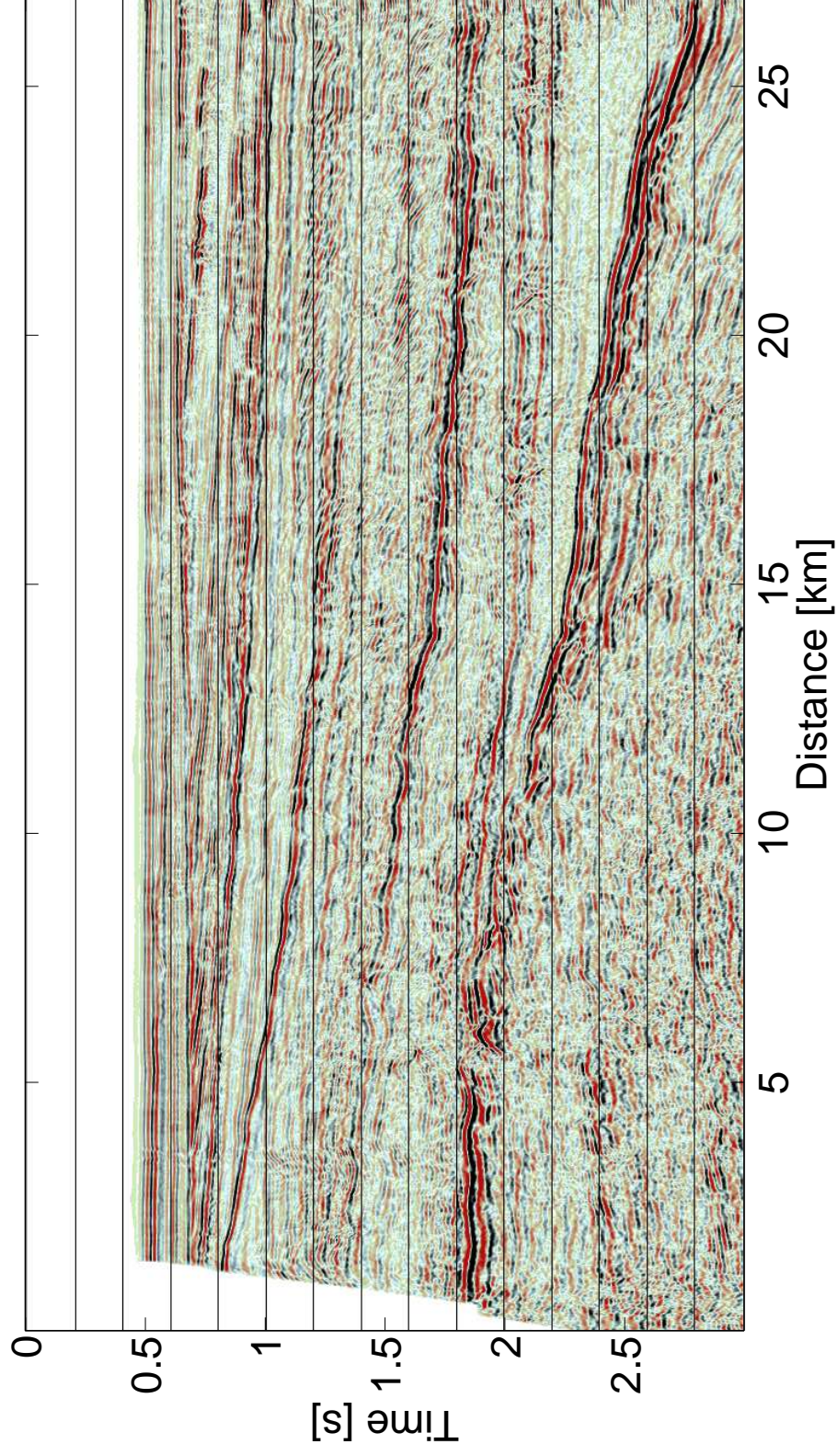
Source: from author

Figure 3.2: Conventional processing. The RMS velocity model.



Source: from author

Figure 3.3: Conventional processing. The NMO stacked section.



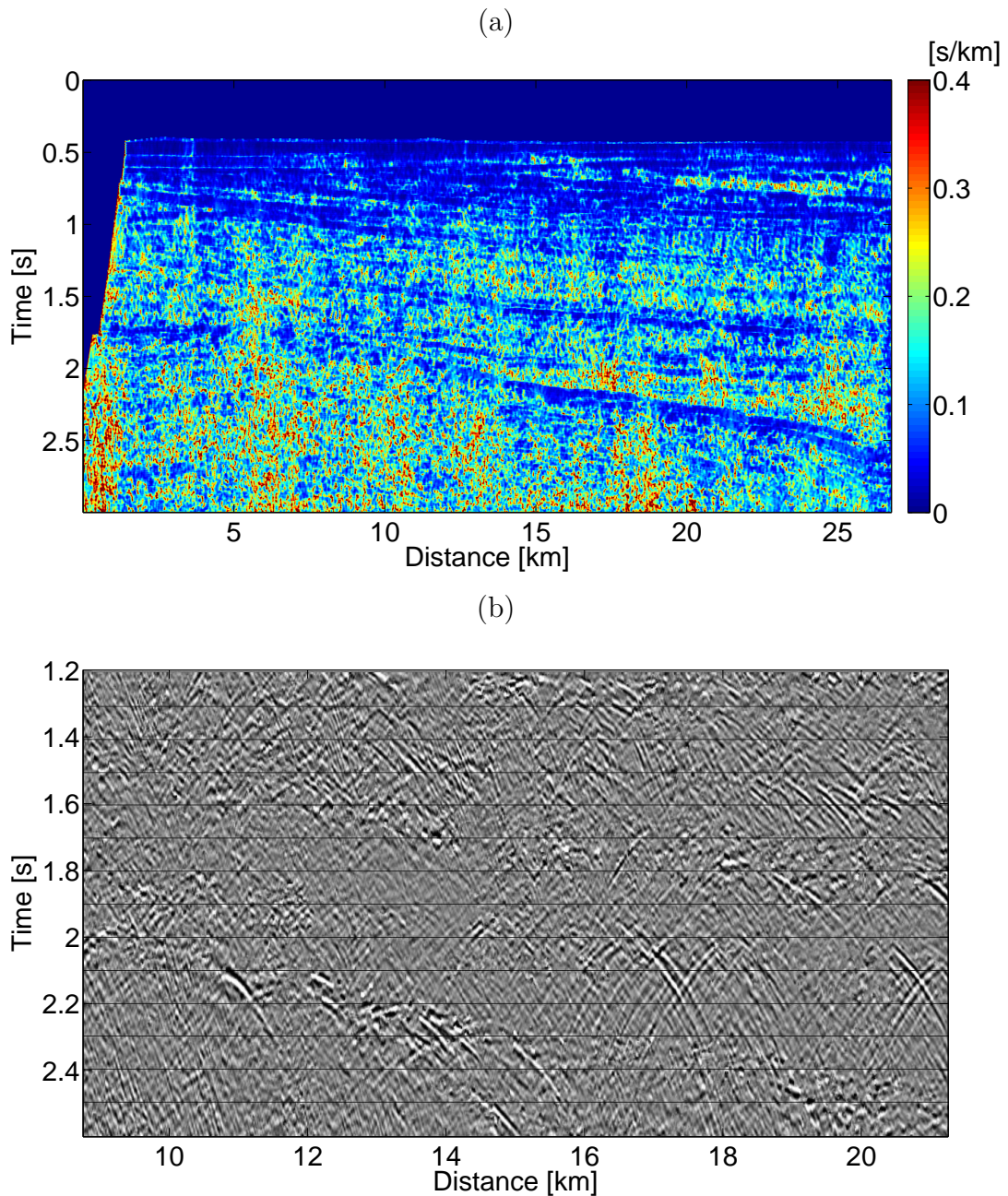
Source: from author

3.3 RDM APPLICATION ON A CONVENTIONAL NMO STACKED SECTION

Before to use the RDM method on near offset, we decided to use the NMO stacked section from conventional processing, to test the RDM method on real data, starting from idea that the NMO stacked section is the most near to ZO section. Therefore we want first to prove the ability of the RDM method working with real data, and the same time, to get velocity model suitable to have a post-stack migration in time.

After obtaining the staked section from conventional processing, we applied the RDM method to this zero-offset section. In this case, the stacked section (approximately a zero-offset section) was the input to the RDM method to obtain a field velocity with diffraction information. After conventional processing we attenuate the reflection event in the stacked section by mean of a PWD filter in order to enhance the diffractions. We, first estimated the local slope (see Figure 3.4a) and following this slope section (input to the PWD) the PWD filter was applied. Figure 3.4b shows the windowed seismic section with diffractions separated.

Figure 3.4: The PWD filter applied on ZO section. (a) Local slopes. (b) Diffraction section.

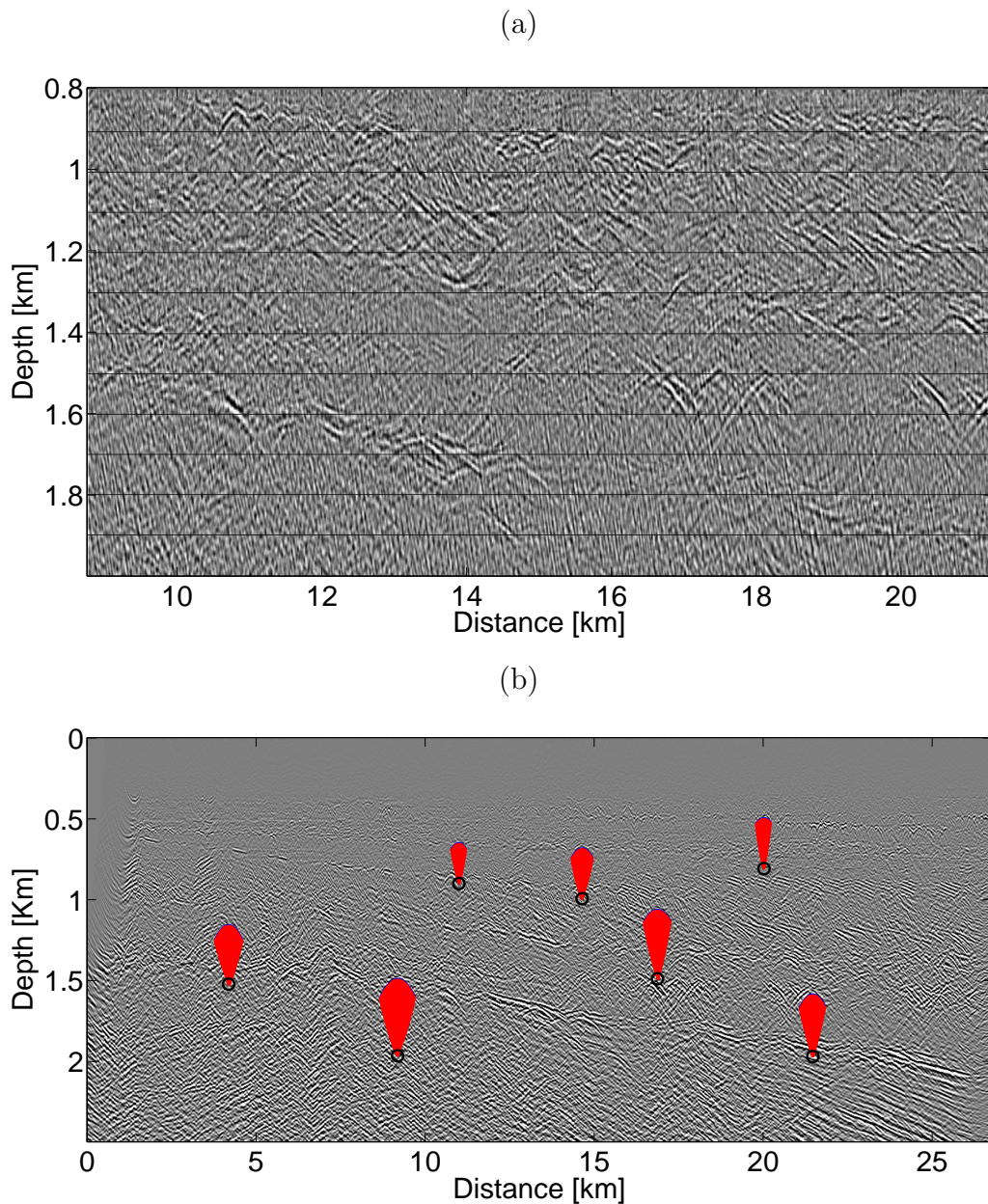


Source: from author

As previously mentioned, the RDM residual diffraction moveout uses the diffraction information to find the velocity models. According to Coimbra et al. (2013), the RDM method requires the diffractions located in depth domain migrated with a constant velocity. Based on this requirement, we performed a depth Kirchhoff migration of the diffraction section using the velocity in water ($v_0 = 1500$ m/s), Figure 3.5a shows different undermigrated diffractions in depth domain. To better visualize the diffractions we windowed the migrated image from 0.8 to 2 km in depth and from 8 to 22 km in the

distance. This depth section was the input to the RDM method. Figure 3.5b shows the remigration trajectories pointing to the correct depth locations.

Figure 3.5: The RDM applied on ZO section. (a) The Depth migration with a velocity $v=1500$ m/s (undermigrated diffraction) of the diffraction section. (b) Remigration trajectories (red lines) for the undermigrated diffractions.

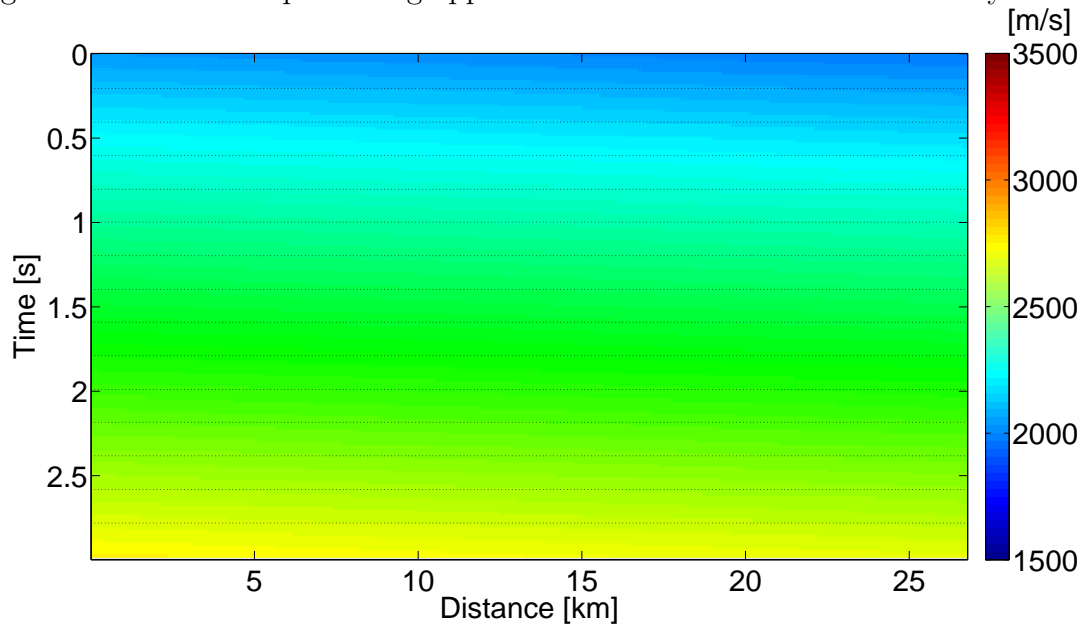


Source: from author

According to Coimbra et al. (2013), we applied the residual diffraction moveout on the undermigrated section, as shown in Figure 3.5a. In general, we selected windows with some diffraction events to locate the diffraction point and to detect the residual moveout. With this information, the velocity v_0 is updated with the assistance of the remigration

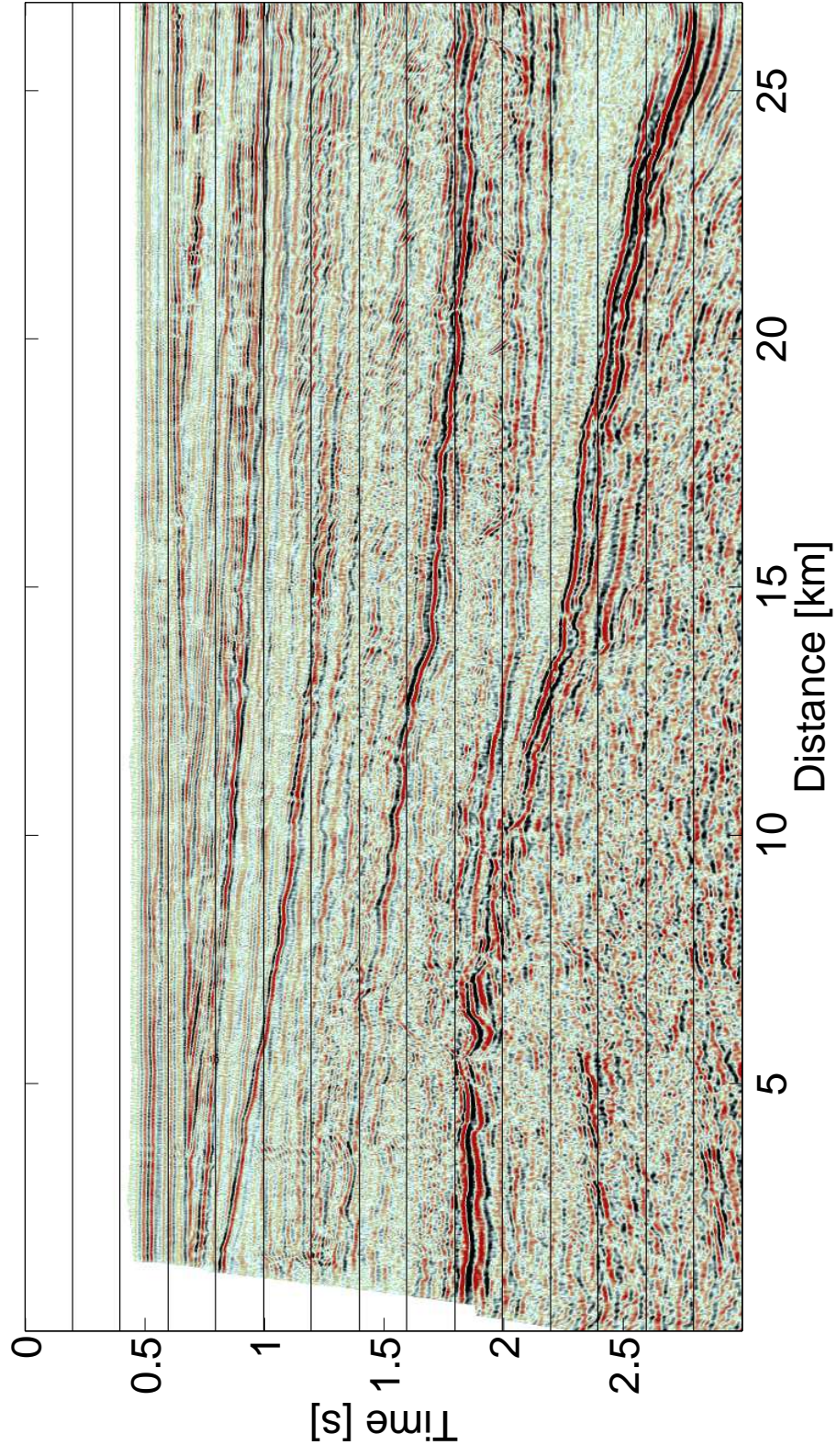
trajectories. Finally, we found an average depth velocity model obtained from the residual diffraction moveout, and then converted it to an RMS velocity model (Figure 3.6). With the updated velocity, we then carried out a post-stack Kirchhoff time migration of the unfiltered stacked section, as shown in Figure 3.7. This result is important because we applied the residual diffraction moveout method to real data (ZO), and the image found had the reflection events well located. However, this just shows that the RDM method is successful with stacked section of real data. Though the stacked section used as the input had a velocity model obtain from conventional processing, therefore, in the next section we will apply our new method to obtain a velocity model using only the diffraction information without known velocity model.

Figure 3.6: The RDM processing applied on ZO section. The RMS velocity model.



Source: from author

Figure 3.7: The RDM processing applied on ZO section. The time migration section.



Source: from author

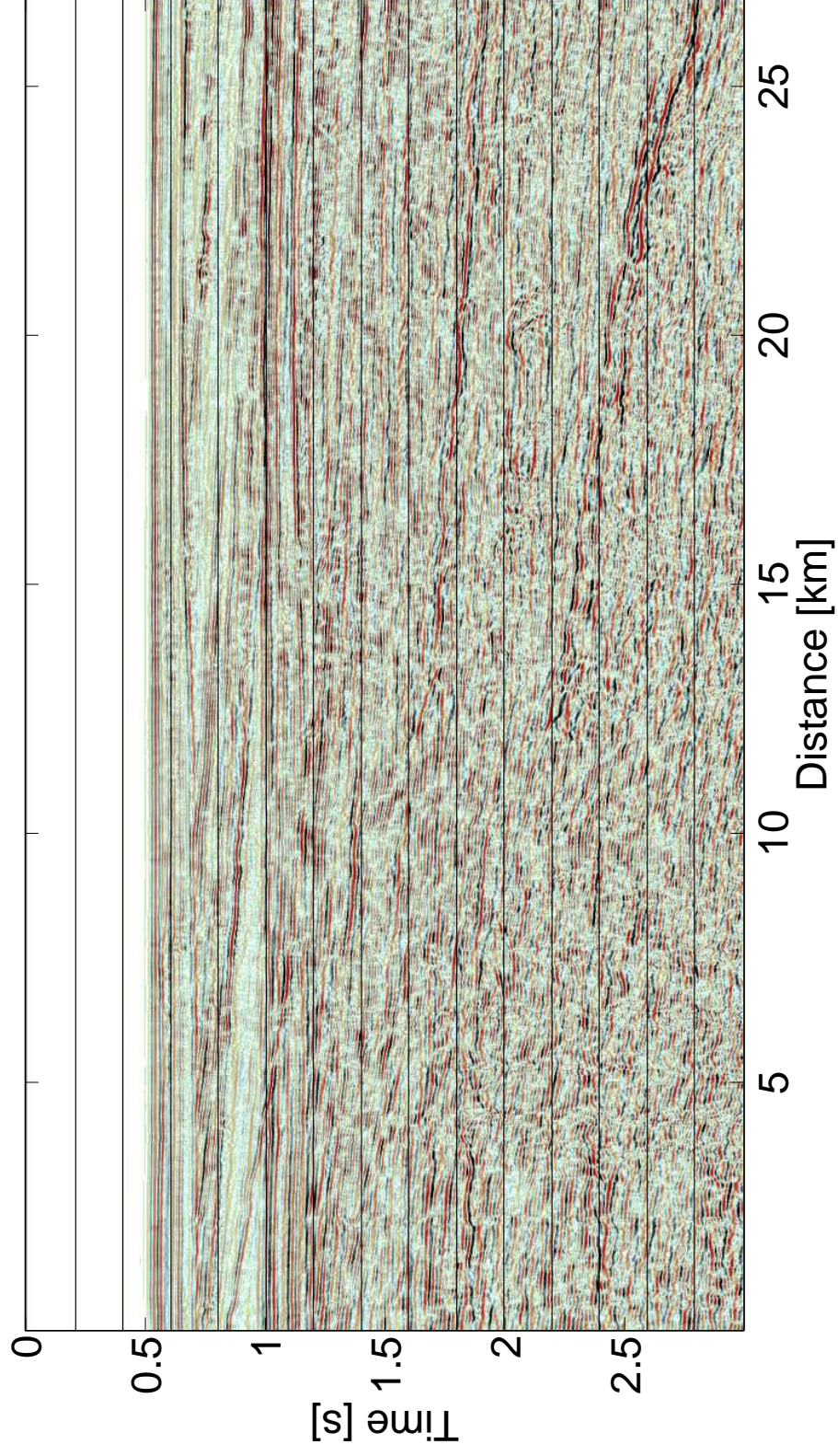
3.4 RDM PROCESSING ON NEAR OFFSET SECTION

After many tests, we finally found a way to apply the residual diffraction moveout (Coimbra et al., 2013) on real data (near offset). Taking in account a suitable data selection, estimating of the local slope, and applying of the PWD filter and the iterative methodology of RDM were fundamental to achieving good results. As mentioned above in this work, what we call the RDM processing to the local slope (σ) estimation, PWD filter application and iterative moveout diffraction. The application of these steps provided velocity model in the time and depth domains. The post-stack time migration, post-stack depth migration and pre-processing were carried out with conventional tools. RDM processing was applied in two parts. The first, we applied the RDM method in a near offset section to obtain the first velocity model which was the input for a NMO stack. The second part is an iterative application of RDM processing. In this case the input to each iteration is the velocity model and NMO stacked section obtained in the previous iteration.

An analytical application of the residual diffraction moveout method requires a zero offset (ZO) section as input parameter (Coimbra et al., 2013). In real data set an approximate zero-offset section is determinate by NMO stacking operation. However, to avoid any error due to the stacking operation, we used the minimum offset section from this data set. In the Viking Graben data set the near offset section is 262 m. We know that if we apply the RDM to a near zero-offset section there will be an error in the velocity model. We hope to correct this error by additional iterations of RDM processing. Figure 3.8 shows near offset section used as the input data. For each subsequent iteration, the input will be the NMO stacked section obtained from the previous iteration.

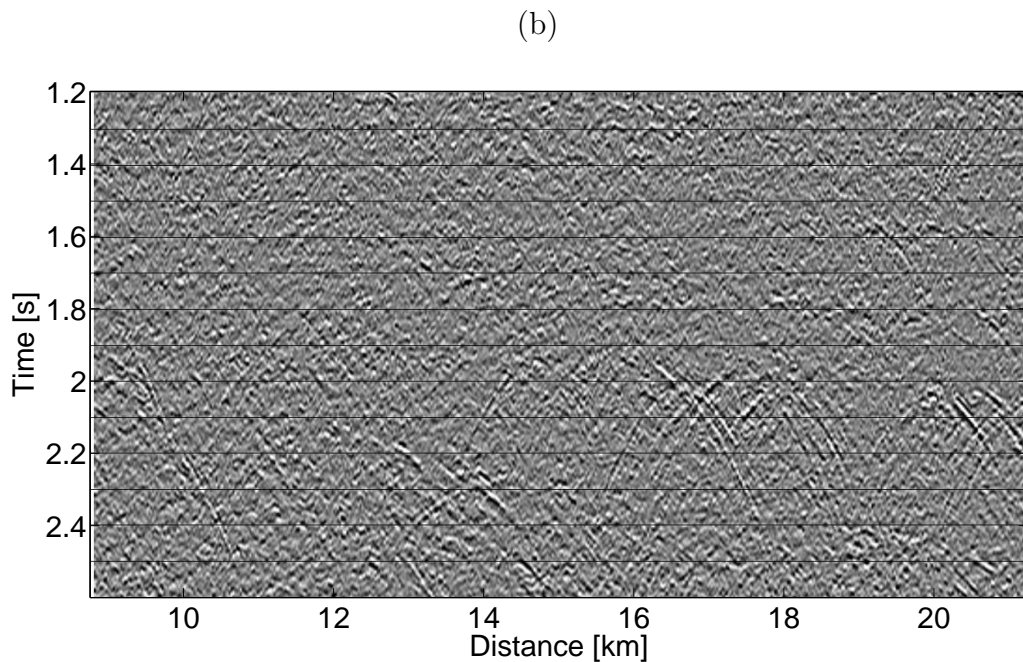
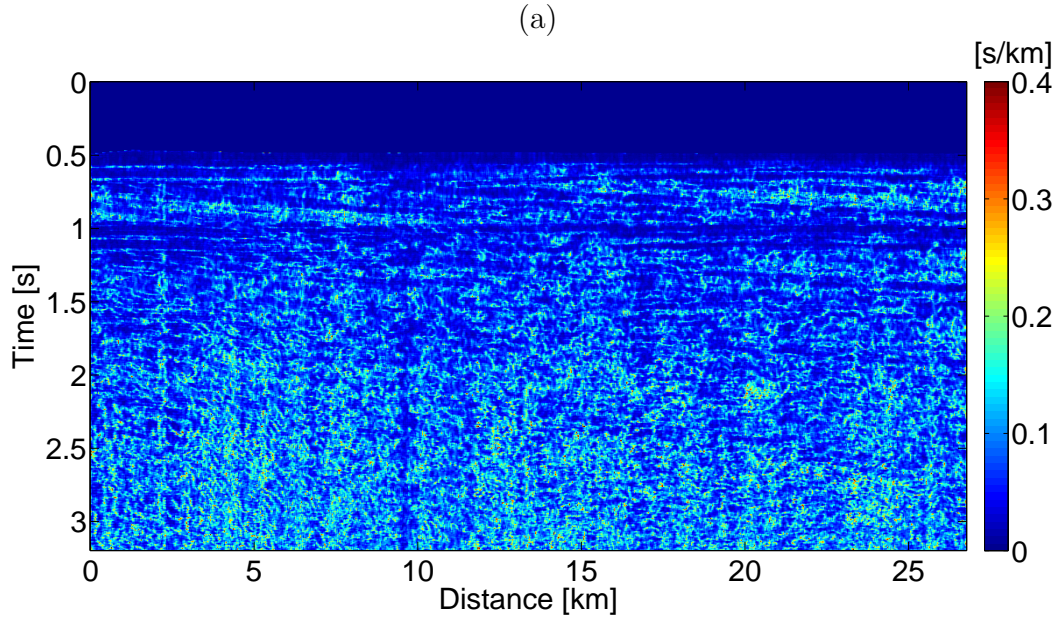
Again, by applying the PWD, we were capable of separating diffractions from reflections as shown in Figure 3.9b. As mentioned earlier, to use RDM processing the local slope must be estimated and used in the PWD filter for each iteration. In an unfiltered near offset section, it is difficult to identify the true diffractions (see Figure 3.8). Figure 3.9a shows the local slopes of the near offset section. This result could be confusing because there is little variation in the slope. If we take a closer look, we can see that the reflection events have a smaller slope value than the potential diffraction events. Therefore, the largest values of the local slopes calculated in the first iteration may indicate zones with possible diffractions (see Figure 3.9b).

Figure 3.8: Near-offset section, which is the input to the first iteration of RDM processing.



Source: from author

Figure 3.9: First iteration of RDM processing. (a) Local slopes panel of a near offset section. (b) Diffraction section, i.e. result of PWD filter applied to near offset section. The window ranges from 8 km to 22 km horizontally and from 1.2 s to 2.6 s in time.

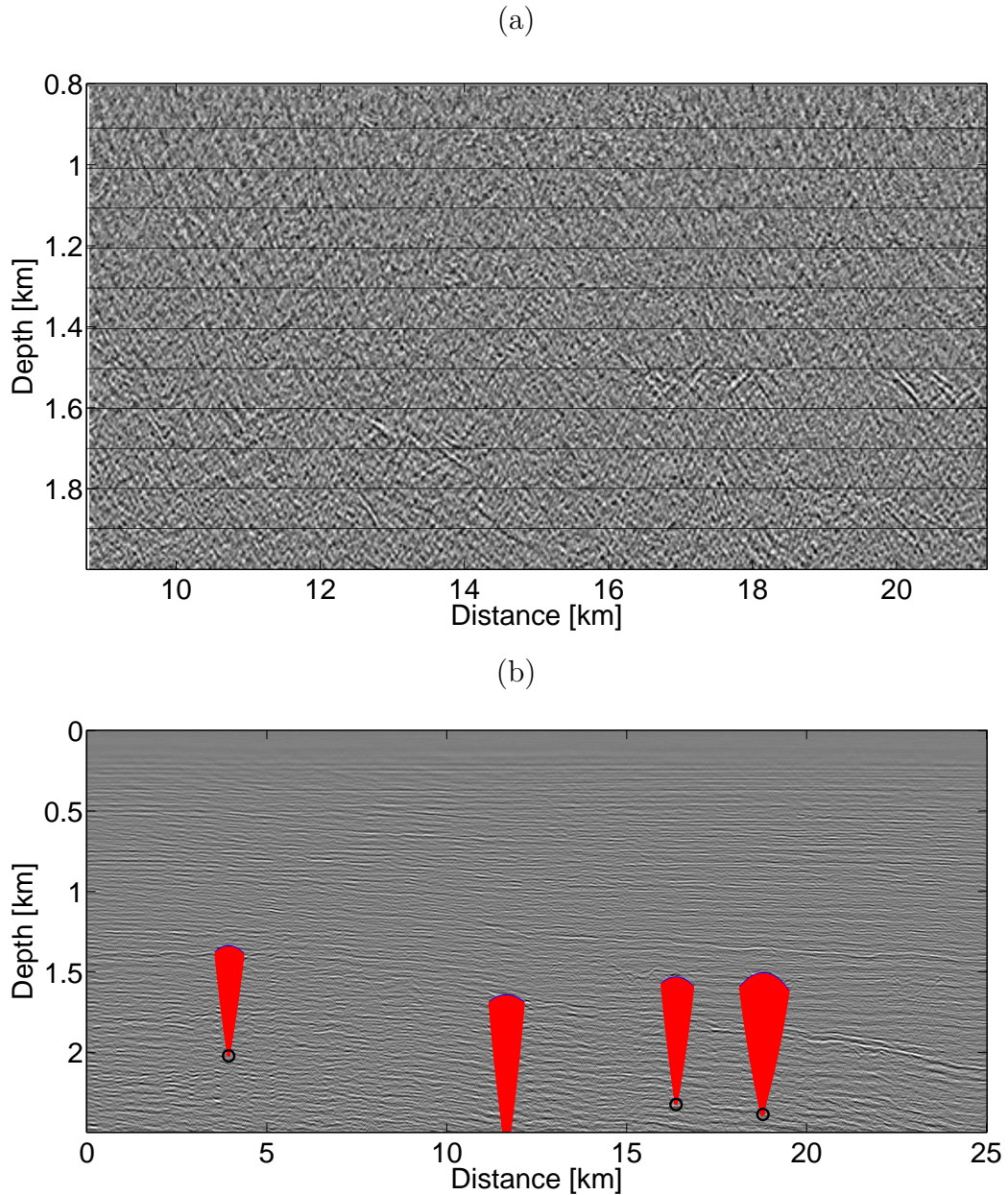


Source: from author

Similar to the way we applied RDM to the NMO stacked section, we performed a depth Kirchhoff migration on the diffraction section shown in Figure 3.10a, using the water velocity ($v_0 = 1500$ m/s), the result shows the different undermigrated diffraction in the depth domain. To better visualize the diffractions, we windowed the migrated image from 0.8 to 2 km in depth and from 8 to 22 km in distance. Figure 3.10b shows the diffraction migrated section with remigration trajectories (red lines) to update the first

velocity v_0 .

Figure 3.10: First iteration of RDM processing. (a) Depth migrated of near offset section with the PWD filter. We assume the initial velocity is water velocity $v = 1500m/s$. (b) Undermigrated filtered diffractions with the remigration trajectories (red lines).

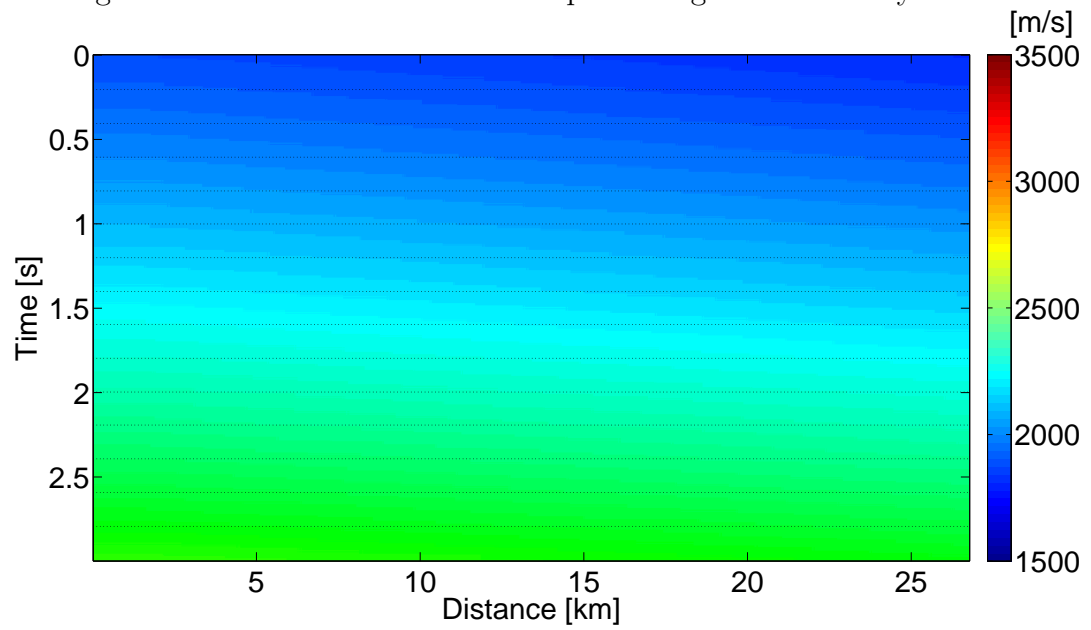


Source: from author

With the updated RMS velocity model (Figure 3.11), we applied the NMO correction and stacked the result to obtain the input to the second iteration (Figure 3.12). As we can see the left side of Figure 3.12, the reflectors are not well positioned. This happened because we did not find diffractions in these regions in the First iteration. But this issue is not important in this stage, because as the velocity model improve new diffraction at

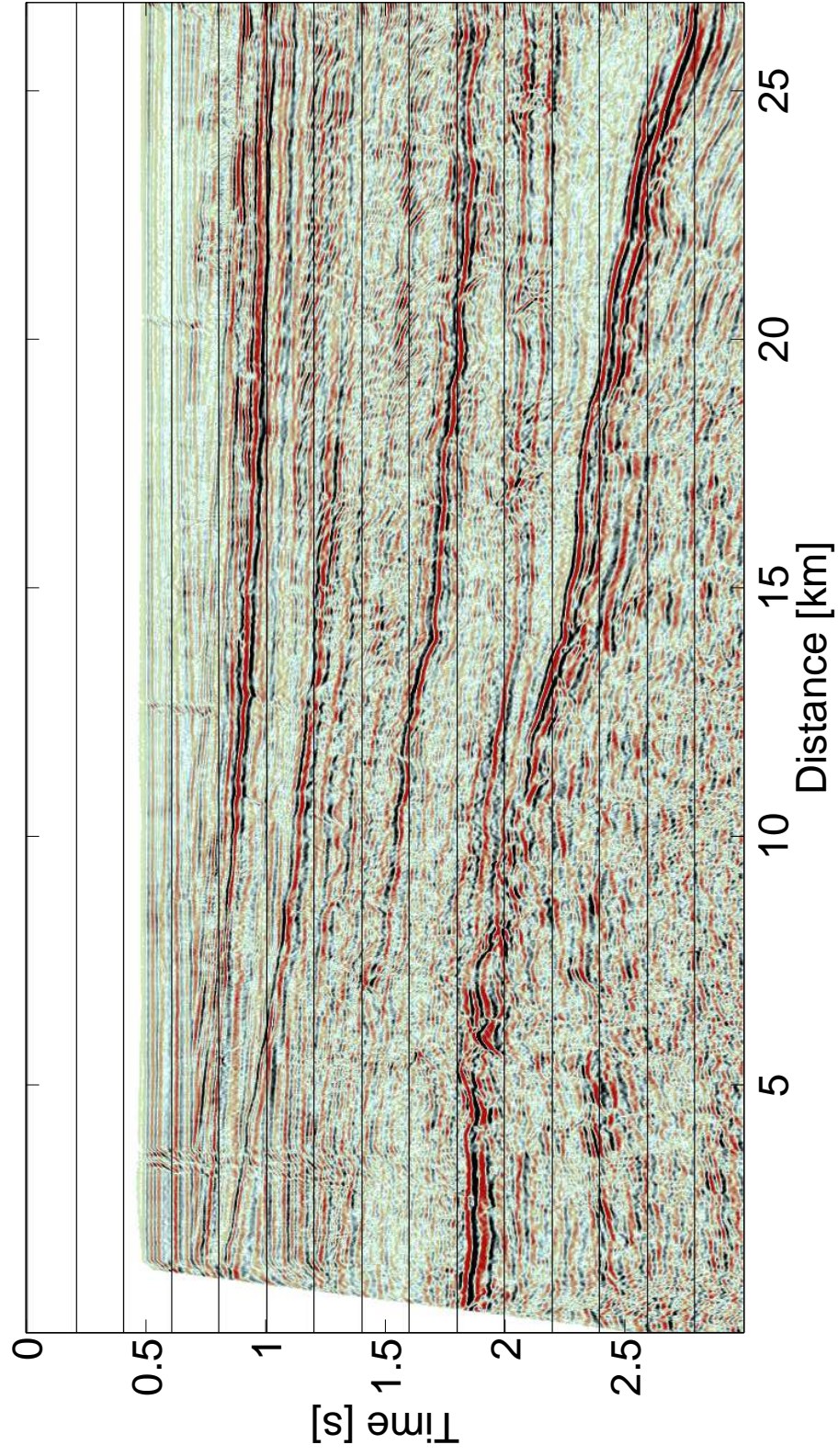
the top of image can be interpreted (see Figure 3.14b).

Figure 3.11: First iteration of RDM processing. RMS velocity model.



Source: from author

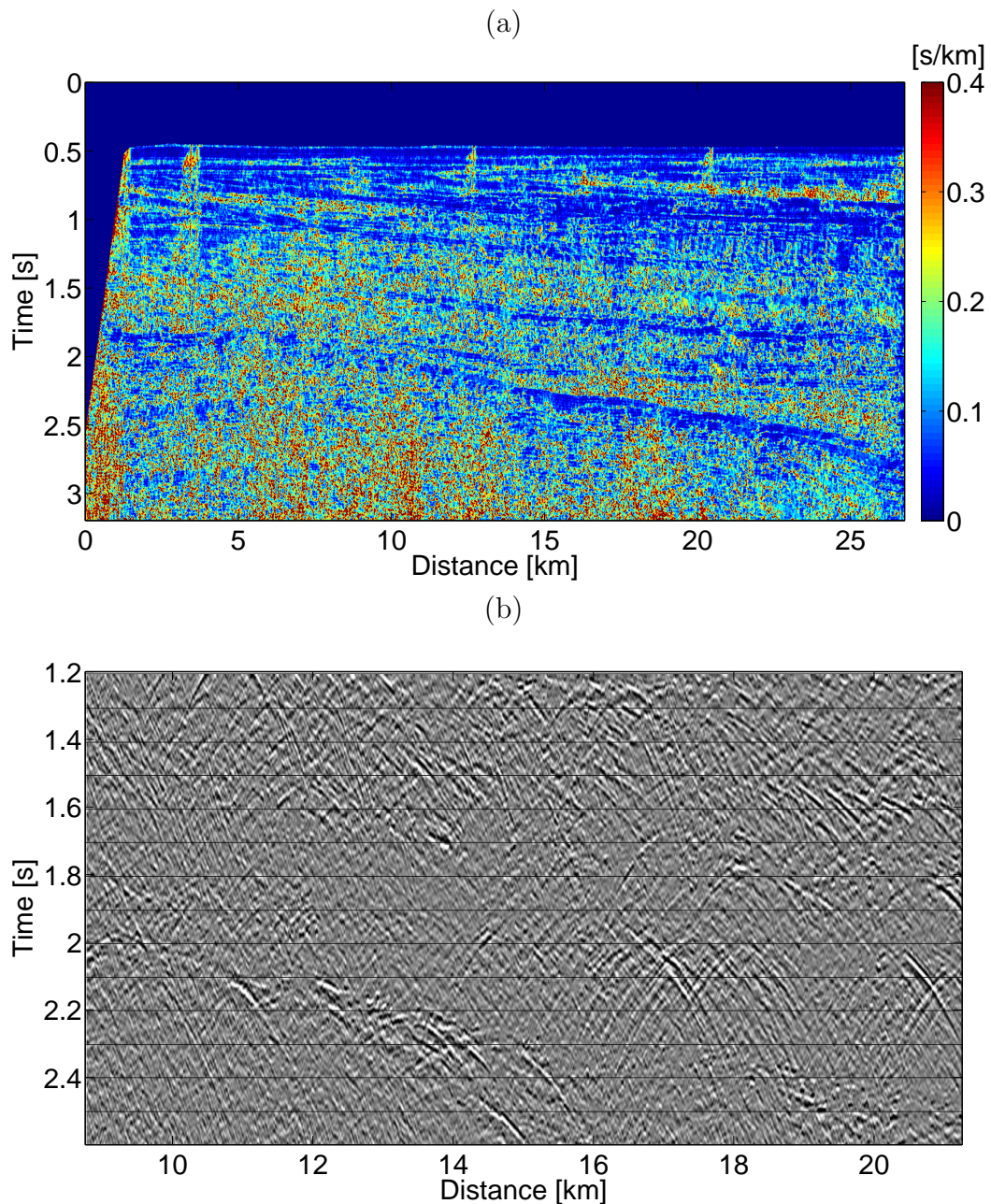
Figure 3.12: NMO stacked section from first iteration of RDM processing. This section is the output from the first iteration and will be the input to the second iteration.



Source: from author

We used the NMO stacked section from the first RDM iteration to estimate the local slope and apply the PWD filter in the second iteration. Figure 3.13a shows the local slope estimated in this new iteration. In this case, unlike the first iteration, we have the necessary information to do a good diffraction filtering, because in the second iteration, some diffraction events are visible (see Figure 3.13b). This will help us correct the error generated in the first iteration (error due to the nonzero offset).

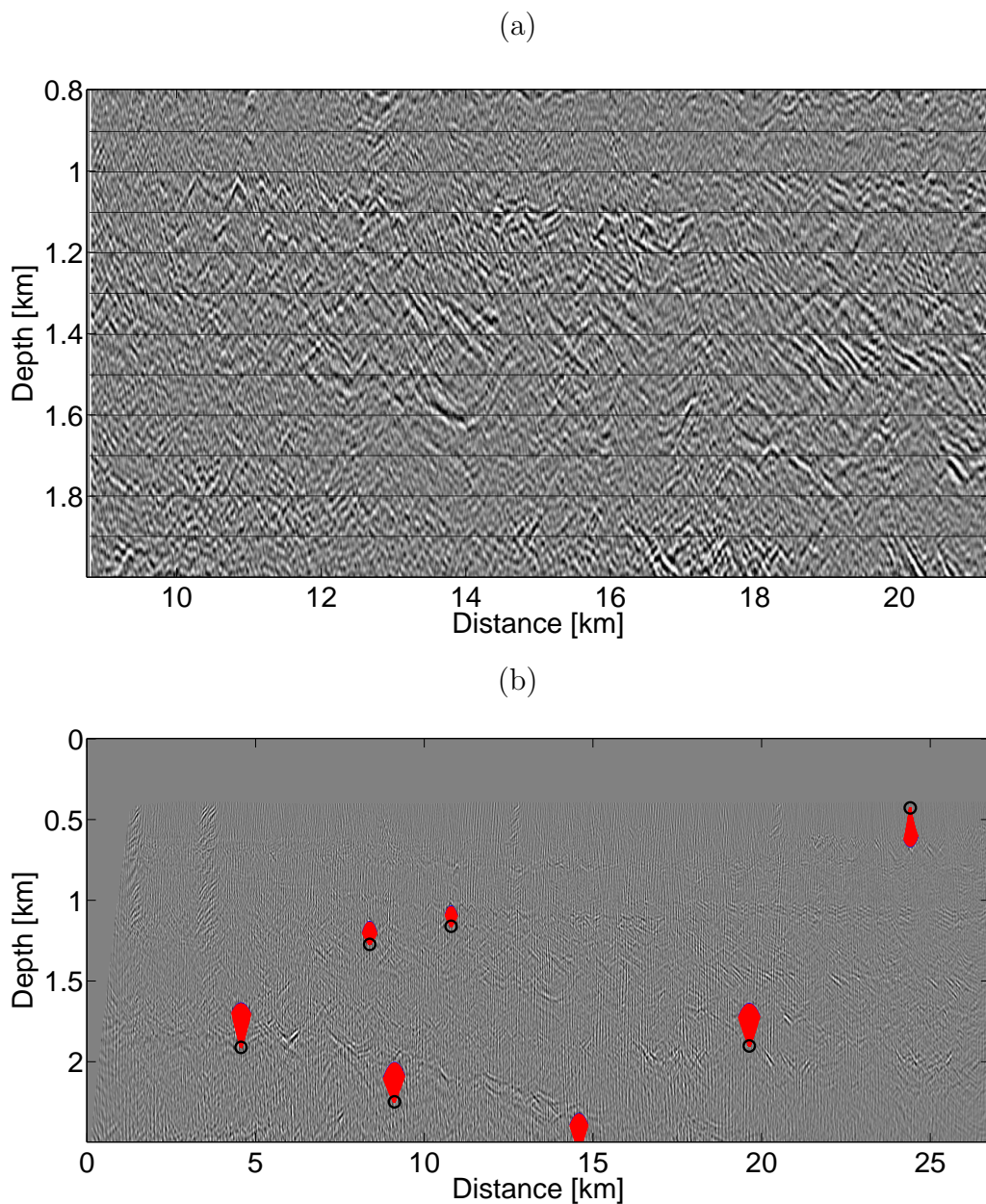
Figure 3.13: Results from second iteration of RDM processing. (a) Local slopes panel of NMO stacked section. (b) Diffraction section, i.e. result of PWD filter applied to the NMO stacked section.



Source: from author

It is very important to observe that in the first iteration, the depth migration is done with a velocity v_0 of 1500 m/s, because we assume that no priori velocity model is known. From the second iteration, on each depth migration of the diffraction panel is performed with the velocity model found in the previous iteration. Figure 3.14 shows the migration image of the diffractions section with the velocity model from the first iteration also showing the migration trajectories (red lines).

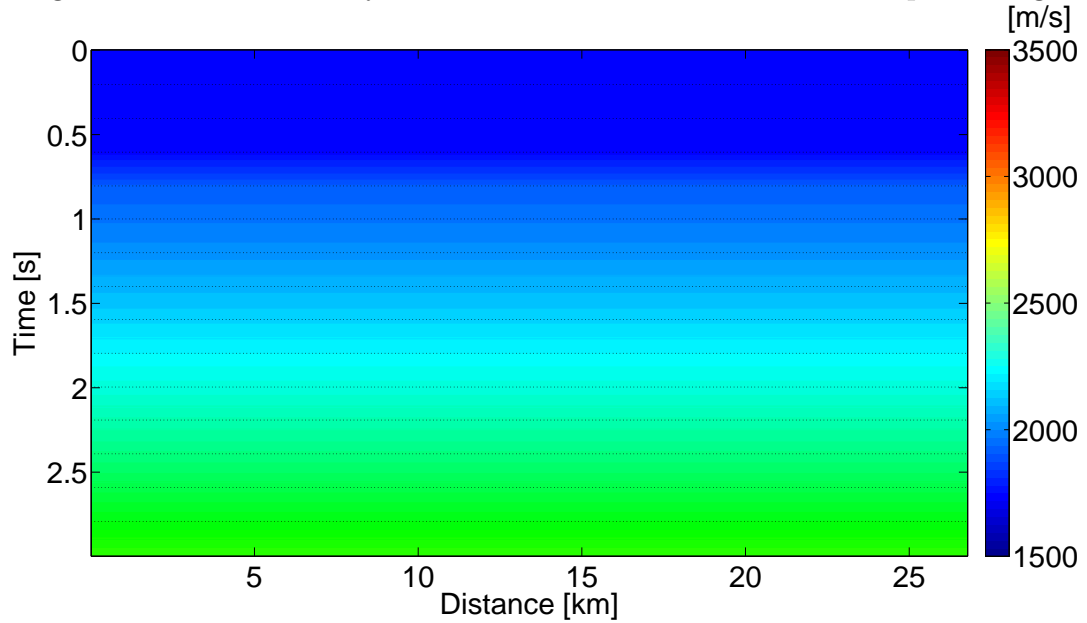
Figure 3.14: Second iteration of RDM processing. (a) Depth migration of diffraction section. This migration was carried out with the velocity model found in the first iteration. (b) Undermigrated diffraction curves with remigration trajectories (red lines).



Source: from author

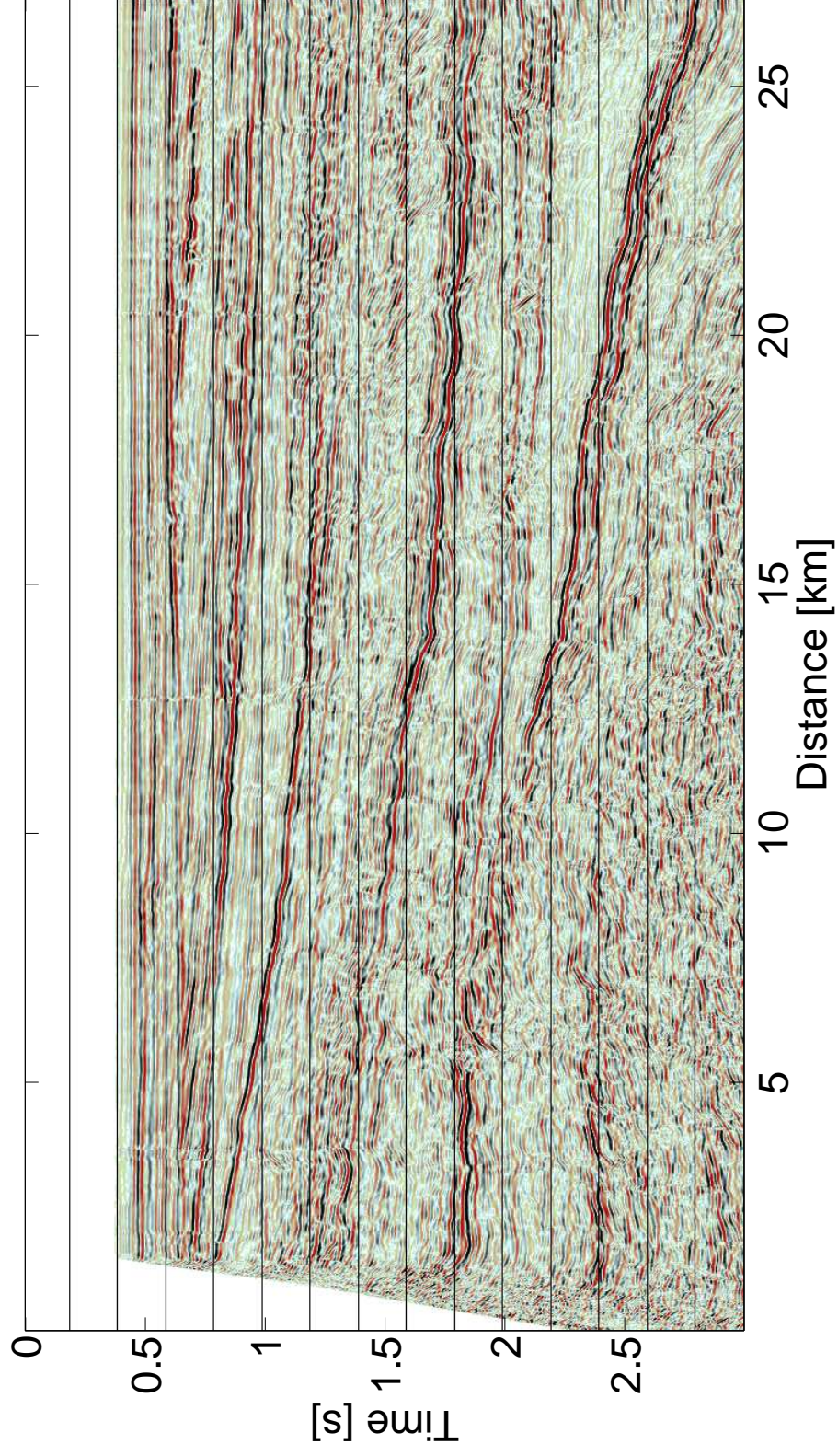
Finally, with the velocity model found in the second RDM iteration (see Figure 3.15) we obtained a new NMO stacked section (Figure 3.16). The error due to the finite offset, has been reduced. This can be deduced from the fact that the events in the top of image have better continuity than in the image of the previous iteration (Figure 3.12)). In other words, the previous error, resulting from stacking at the near offset section, was overcome after two iterations.

Figure 3.15: RMS velocity model from second iteration of RDM processing.



Source: from author

Figure 3.16: NMO stacked section from second iteration of RDM processing.

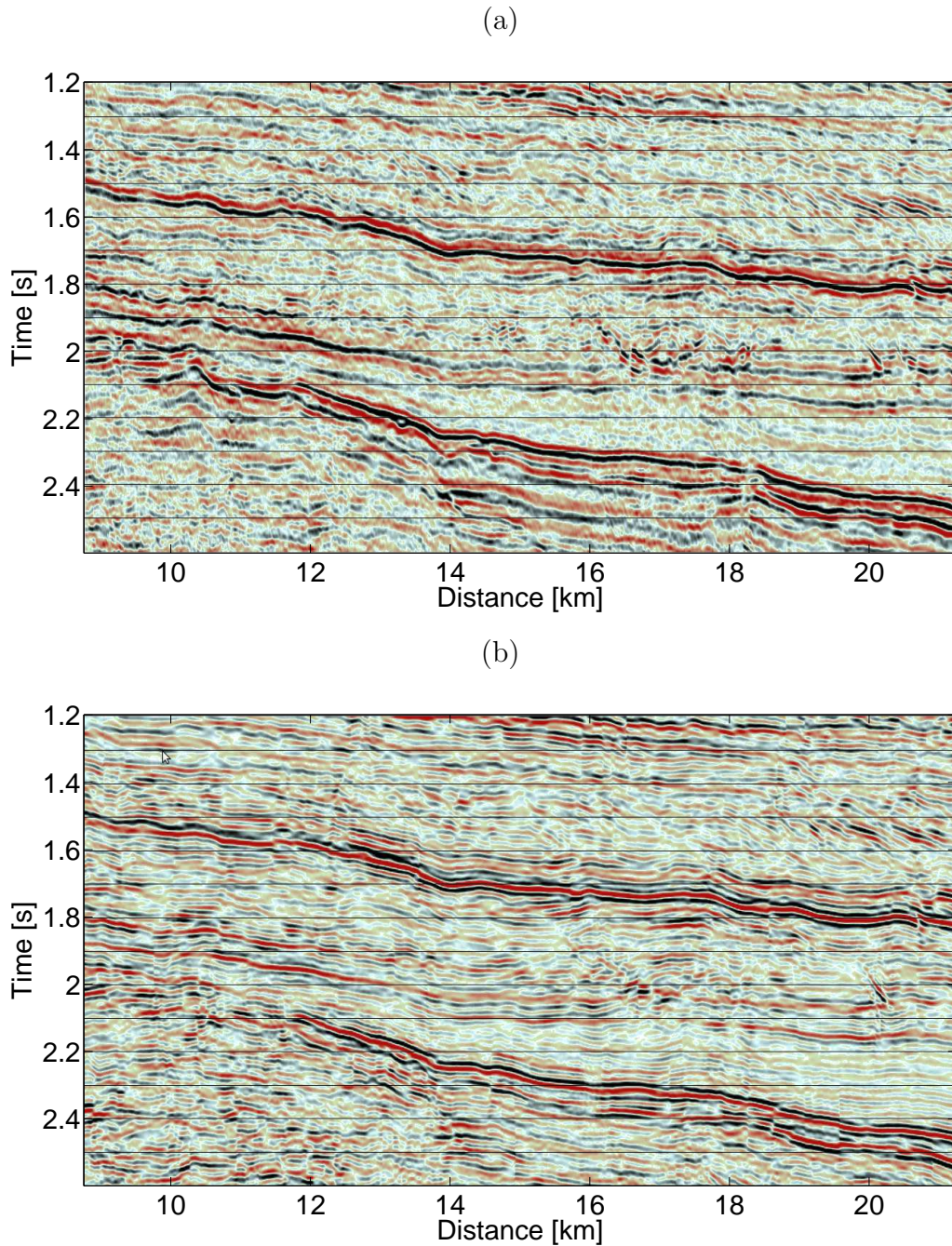


Source: from author

After establishing the velocity models in the time and depth domains using the conventional velocity analysis and the RDM processing, we performed a post-stack Kirchhoff migration operation in the time and depth domains. In both cases, we used a maximum frequency of 50.0 Hz for migration. The same parameters for the time and depth migrations were used for the RDM and the conventional processing. The seismic images were windowed for better visualization.

Figure 3.17 shows the post-stack time migrated sections. As can be noted, the results were quite similar. However the velocity model obtained from RDM and conventional velocity processing presented some differences. Figure 3.17a shows time migrated image using the velocity image from conventional processing. This image shows continuous reflectors. However, the local lateral variation of reflectors are quite wrong, and the information after 2.2 s and in the first 12 km have a low coherence. In contrast, the time migration with the RDM velocity (Figure 3.17b) shows a good energy distribution with a smooth local lateral variation, and the reflection below 2.2 s are better imaged. For reference the time migrated image from Gislain & McMechan (2003).

Figure 3.17: Time migrated sections with the velocity model from (a) the conventional processing and (b) RDM processing. The images were windowed horizontally (from 0.8 to 22 km) and in time (from 1.2 to 2.6 s) for better visualization.

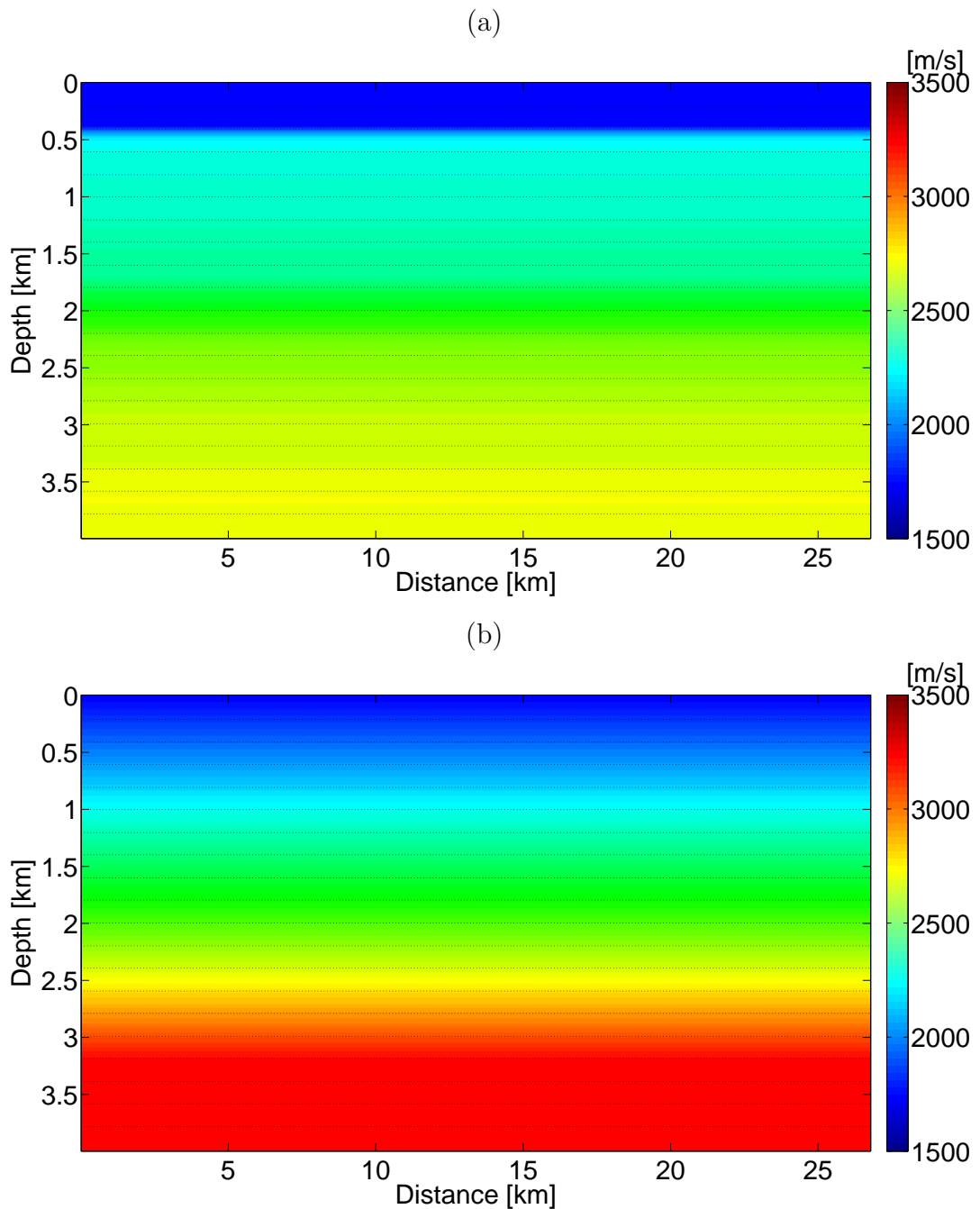


Source: from author

Figure 3.18 shows the depth velocity models from conventional and RDM processing. The average velocity from the RDM method was converted for interval velocity using Schleicher et al. (2004). The interval velocity in the conventional processing was obtained from Dix conversion (by PROMAX). In both cases, no lateral variations are taken into account. However, the velocity from RDM processing has a better correlation with layers

in the seismic section than the conventional velocity. Another difference is the value of the velocity at the depths greater than 2 km. It can be noted that the RDM velocity increases faster than the conventional velocity. This behavior has an effect on the position of the reflectors in depth migration. The conventional model can be enhanced to find a better correlation with the layers, but that will require more run time compared with RDM processing.

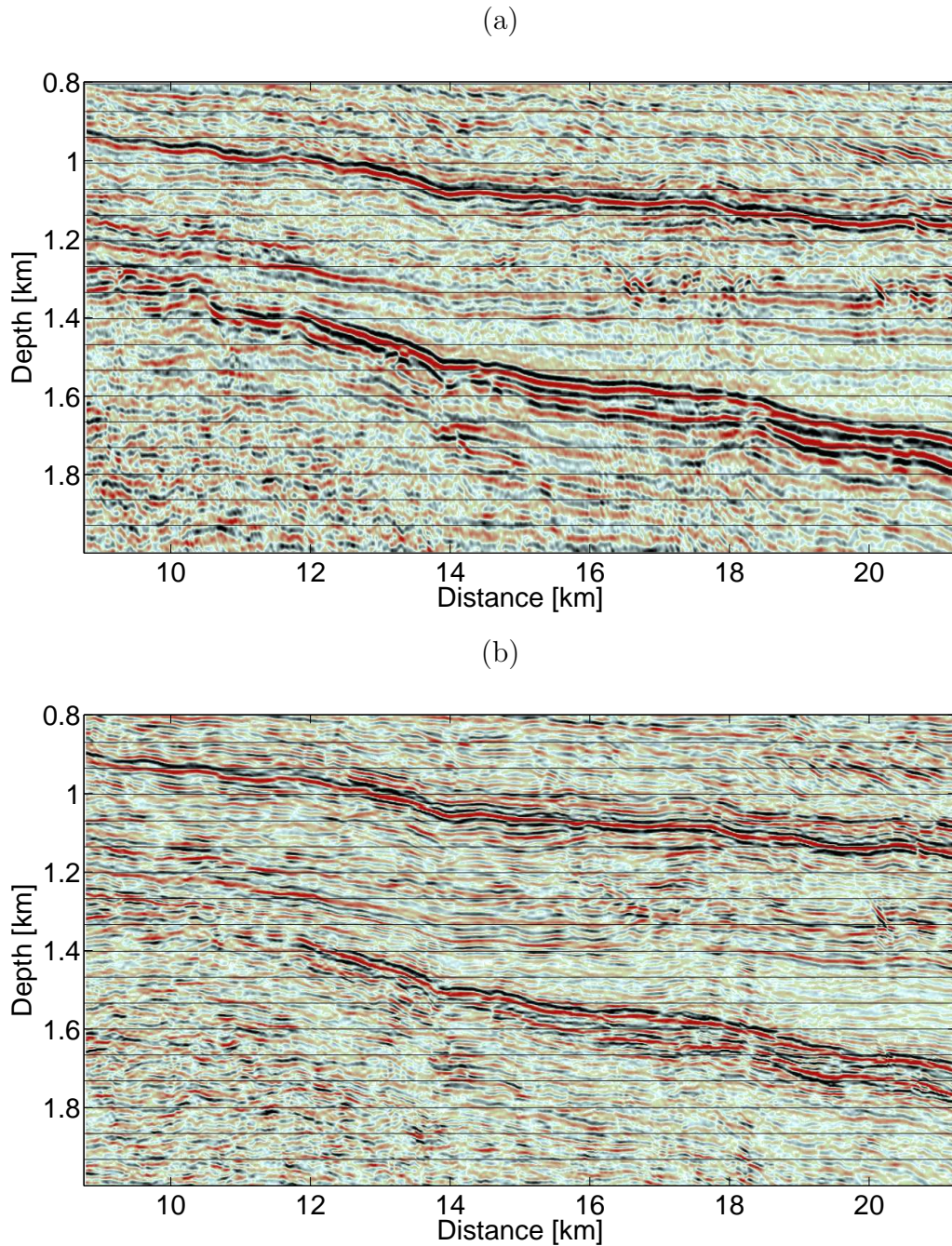
Figure 3.18: Final depth velocity models from (a) conventional and (b) RDM processing.



Source: from author

With the velocity models in the depth domain from the RDM and conventional processing, we performed a depth migration (Figure 3.19a and b). This depth migration has little different in the structures, although one actual variation is the position of the reflectors in depth. Furthermore, the Figure 3.19b shows a well location of faults in lower layer of section. This indicates that the velocity model found in the second iteration of the RDM processing give us a good velocity model in depth.

Figure 3.19: Depth migration sections using interval velocity model from (a) conventional processing and (b) RDM processing. The images were windowed horizontally (from 0.8 to 22 km) and in depth (from 1.2 km to 3.0 km).



Source: from author

Note that the main goal of work relay on into proposes a different way to improve velocity models in the time and depth domains. It is very probable that some parameters can be better adjusted for this unconventional RDM processing. New tests could be made with other local slope estimation, another method to filtering diffractions from reflections

and new ways to interpolate the velocity values obtained from local diffractions. In this simple real data set, the application of RDM was considerable faster due the small number of picked diffraction points (eleven) required to reach a suitable velocity model. However, in a complex data set or 3D data, the manual picking is very costly. In this situation automatic picking can be a suitable way to construct velocity model using RDM processing.

4 CONCLUSIONS

In this paper we have compared the seismic migrated images obtained by conventional seismic processing with migrated images obtained by a new processing sequence based on the RDM technique developed by Coimbra et al. (2013). Although this technique had been developed for ZO sections, the error produced in applying a method developed for ZO section to near-offset profile was overcome after two iterations. We have shown here, that for near offset sections from the Viking Graben seismic data, only two iterations were sufficient to overcome the near offset problem and produce acceptable velocity models for time and depth migration.

In addition we have implemented a modified PWD filter. In this filter version, we have used the local slope technique together with the PWD filter to better separate diffraction from reflections. This step was very important in this analysis, in view of the weak energy of diffraction compared with the energy of reflections and sometimes even the noise. Because of the large energy difference, To identify diffractions in a real data set is a difficult task in seismic processing.

As our results showed, the velocity models in the time and depth domains obtained from RDM processing produced an acceptable seismic section comparable to the conventional method. The important difference in this case was the time it took to construct the velocity model. The time spent to achieve an acceptable migration-velocity model was significantly less than the time used to obtain a velocity model based on semblance analysis. For the Viking Graben data set, we produced a satisfactory migration-velocity model in 1 day approximately, while the conventional semblance analysis took four days.

It is important to emphasize that we do not aim to suggest that our methodology is better or worse than conventional methodologies. We are simply considering the possibility to construct velocity models based on diffractions, which was feasible in the case of the Viking Graben data set. Furthermore, it is known that it is hard to quantify the seismic processing time, especially when the time depends on the human interaction. However, in our case, as commented by Coimbra et al. (2013), RDM has a very low computational cost. Regarding the time to generate a velocity model based on RDM, most of the time required to reach an applicable velocity model is spent on identifying the diffractions. However, here, the diffraction filtering before applying RDM saved time in the processing.

The RDM processing has some aspects that can be improved in future research, mainly, in the improvements in handling velocity models and the interpolation method of velocity models. An automatic diffractions (de Figueiredo et al., 2013) identification before the diffraction picking will improve the performance of residual diffraction moveout processing. With this improvements are expected to reduce the processing time and the human error.

BIBLIOGRAFIA

- Alonaizi, F.; Pevzner, R.; Bóna, A.; Alshamry, M.; Caspari, E.; Gurevich, B. Application of diffracted wave analysis to time-lapse seismic data for CO₂ leakage detection. *Geophysical Prospecting*, v. 62, n. 2, p. 197–209, 2014.
- Alonaizi, F.; Pevzner, R.; Bóna, A.; Shulakova, V.; Gurevich, B. 3D diffraction imaging of linear features and its application to seismic monitoring. *Geophysical Prospecting*, v. 61, n. 6, p. 1206–1217, 2013.
- Asgedom, E.G.; Gelius, L.J.; Tygel, M. Diffraction separation using the crs technique: A field data application. Twelfth International Congress of the Brazilian Geophysical Society, Brazilian, 2011.
- Clearbout, J.F. Earth soundings analysis—processing versus inversion. Blackwell Scientific Publications, 1992.
- Coimbra, T.A.; de Figueiredo, J.J.S.; Schleicher, J.; Novais, A.; Costa, J.C. Migration velocity analysis using residual diffraction moveout in the poststack depth domain. *Geophysics*, v. 78, n. 3, p. S125–S135, 2013.
- de Figueiredo, J.; Oliveira, F.; Esmi, E.; Freitas, L.; Green, S.; Novais, A.; Schleicher, J. Automatic detection and imaging of diffraction points using pattern recognition. *Geophysical Prospecting*, v. 61, p. 368–379, 2013.
- Fomel, S. Applications of plane-wave destruction filters. *Geophysics*, v.67, p.1946–1960, 2009.
- Fomel, S.; Landa, E.; Taner, M.T. Post-stack velocity analysis by separation and imaging of seismic diffractions. *Geophysics*, v. 72, p. U89–U94, 2007.
- Gislain, B.M.; McMechan, G.A. Processing, inversion, and interpretation of a 2d seismic data set from the north viking graben, north sea. *Geophysical Prospecting*, v. 68, n. 3, p. 837–848, 2003.
- Hubral, P.; Tygel, M.; Schleicher, J. Seismic image waves. *Geoph. J. Int.*, n. 125, p. 431–442, 1996a.
- Hubral, P.; Tygel, M.; Schleicher, J. Seismic image waves. *Geoph. J. Int.*, n.125, p.431–442, 1996b.

- Khaidukov, V.; Landa, E.; Moser, T.J. Diffraction imaging by focusing-defocusing: An outlook on seismic superresolution. *Geophysics*, v. 69, n. 6, p. 1478–1490, 2004.
- Klokov, A.; Fomel, S. Separation and imaging of seismic diffractions using migrated dip-angle gathers. *Geophysics*, v. 77, p. S131–S143, 2013.
- Landa, E.; Keydar, S. Seismic monitoring of diffraction images for detection of local heterogeneities. *Geophysics*, v. 63, p. 1093–1100, 1998.
- Landa, E.; Reshef, M. Separation, imaging, and velocity analysis of seismic diffractions using migrated dip-angle gathers. 79th Ann. Internat. Meeting, SEG, Expanded Abstracts, p. 2176–2180, 2009.
- Landa, E.; Shtivelman, V.; Gelchinsky, B. A method for detection of diffracted waves on common-offset sections. *Geophysical Prospecting*, v. 35, p. 359–374, 1987.
- Liu, T.; Hu, J.; Wang, H. Diffraction wavefield separation and imaging using singular spectrum analysis. 78th EAGE Conference and Exhibition incorporating SPE EU-ROPEC, London UK, p. 10–13, 2013.
- Novais, A.; Costa, J.; Schleicher, J. GPR velocity determination by image-wave remigration. *Journal of Applied Geophysics*, v. 65, p. 65–72, 2008.
- Sava, P.; Biondi, B.; Etgen, J. Wave-equation migration velocity analysis by focusing diffractions and reflections. *Geophysics*, v. 70, n. 3, p. U19–U27, 2005.
- Schleicher, J.; Costa, J.C.; Santos, L.T.; Novais, A.; Tygel, M. On the estimation of local slopes. *Geophysics*, v. 74, p. 25–33, 2009.
- Schleicher, J.; Novais, A.; Munerato, F. Migration velocity analysis by depth image-wave remigration: First results. *Geophysical Prospecting*, v. 52, p. 559–573, 2004.
- Zhang, R. *Imaging the earth using seismic diffractions*, 2004.